Modeling Jet Interactions with the Ambient Medium

J.H. Beall[1,2,3]
John Guillory[2], and
D.V. Rose[4]
1. Space Sciences Division, NRL,
Washington, DC,
2. College of Science, GMU, Fairfax, VA
3. St. Johns College, Annapolis, MD,
and
4. Voss Scientific, Albuquerque, NM.

We acknowledge our colleagues:
Mike Wolf, SSD/NRL, Washington, DC,
Kinwah Wu and Curtis Saxton, Mullard Space Sciences Laboratory, London, England.
S. Schindler and W. Kapferer, *Institut fur Astrophysik, Unversitat, Innsbruck,Austria*
S.. Colafrancesco, *Witwaterstnand University, South Africa*

Jets and the central engine of an AGN:

- AGN Schematic showing the accretion torus with the Broad Line Region (BLR) clouds orbiting around the black hole and the accretion disk, the Narrow Line Region (NLR), and the jet of material propagating through central region and outward.

- Cen A core (below) from R. Kraft et al. 1999, 2000 Chandra observations.

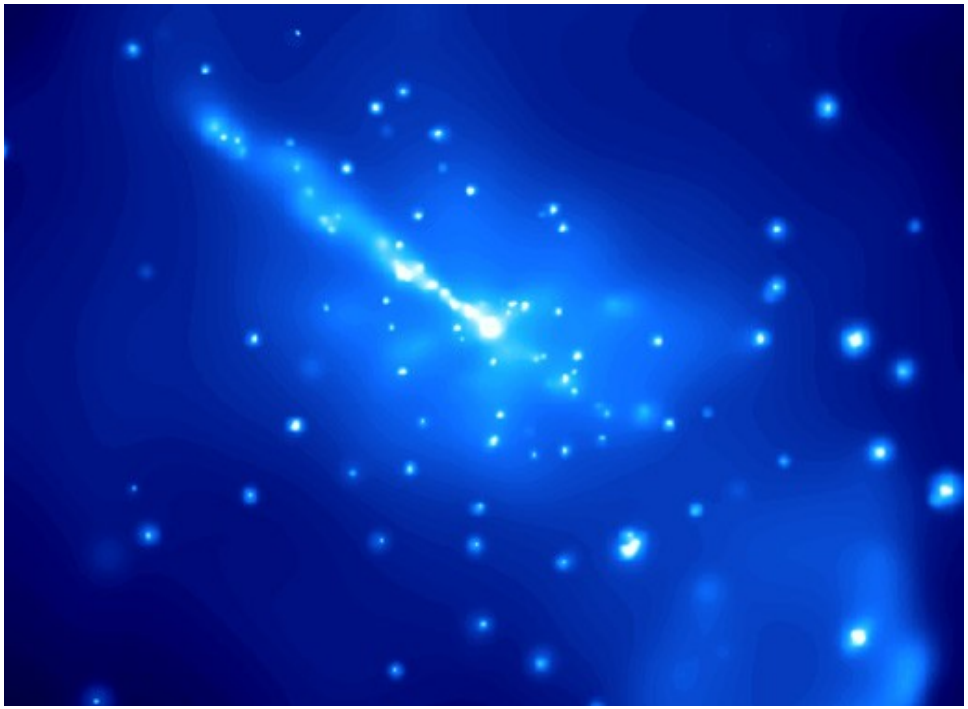

AGN schematic

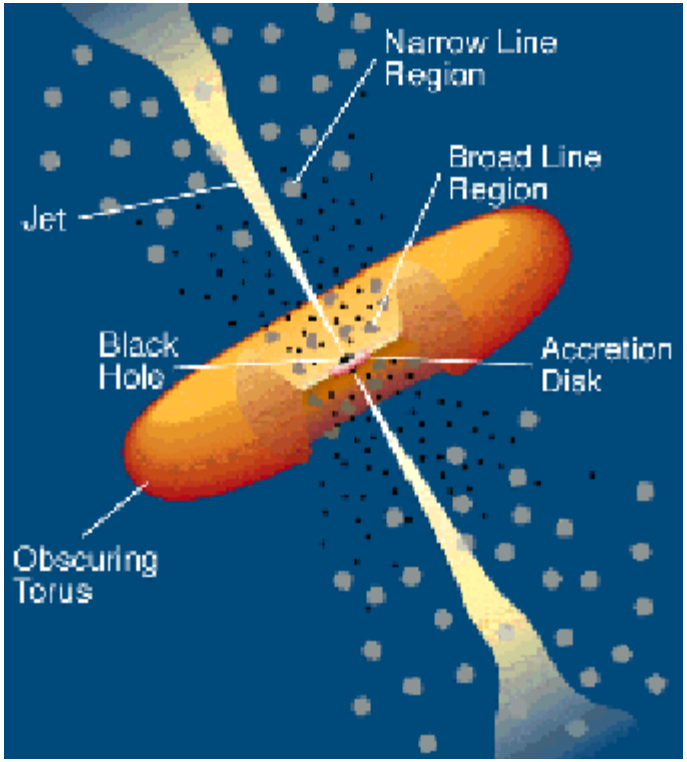

Detectors of comparable resolutions yield a multi-frequency image of M87 jet structure

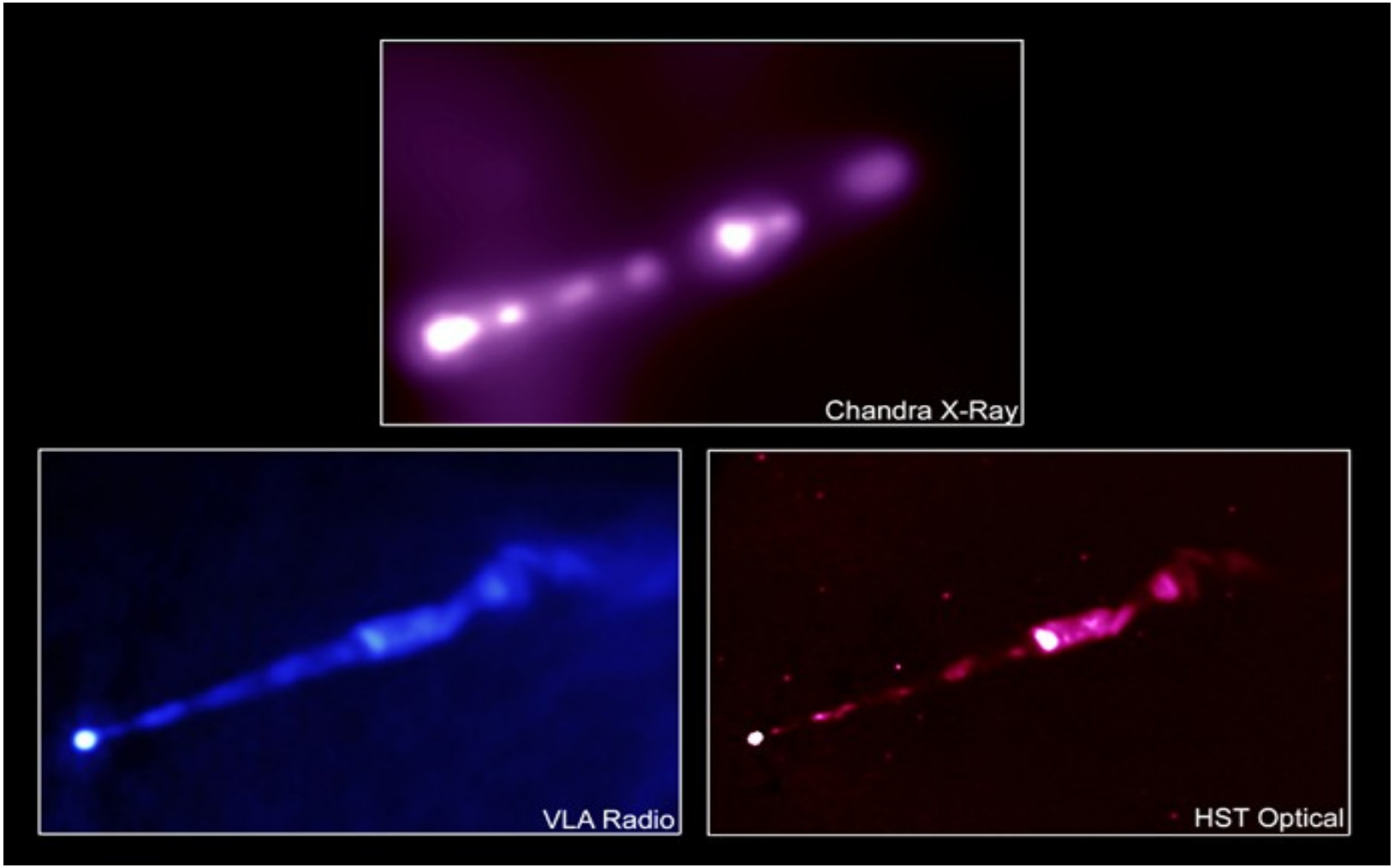

M87 at mas resolution (white bar is .01 pc)

Junor, Biretti, and Livio, Nature 1999, 401, 892

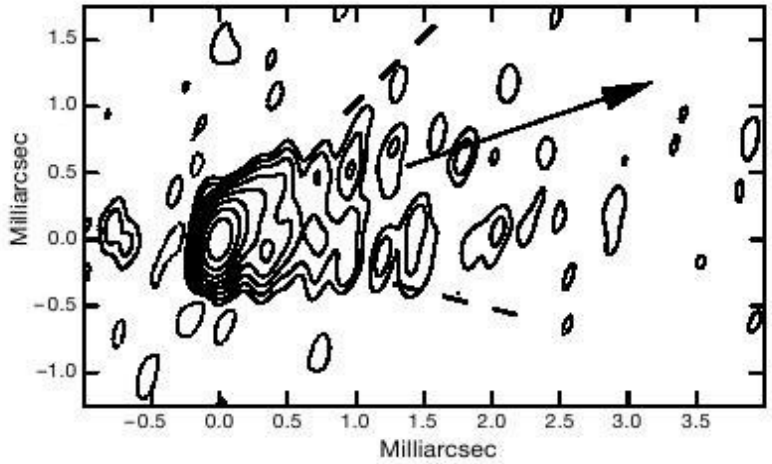

Figure 1 Image of the nucleus of M87 at 43.237 GHz on 3 March 1999. The synthesized beam is 0.33 mas × 0.12 mas (1 mas is 0.071 pc at the distance of M87) with the major axis in position angle −12.3°. The peak brightness in the image is 228 mJy per beam and the r.m.s. noise in the image well away from the bright structure is 0.38 mJy per beam. Contours are plotted at −1, 1, 2, 4, 8, 16, 32, 64 and 128 mJy per beam. The solid arrow indicates the direction of the 20″ jet, while the dashed lines indicate the position angles of the limb-brightened structure within 1 mas of the core. The antenna array consisted of the 10 telescopes of the Very Long Baseline Array (VLBA), 13 telescopes of the Very Large Array (VLA) phased together, and telescopes located at Effelsberg (Germany), Medicina (Italy), Metasahovi (Finland), Onsala (Sweden) and Yebes (Spain). Left circular polarization data were recorded at each telescope using 8 channels of 8 MHz bandwidth and 2 bit sampling. The data were correlated at the VLBA correlator, and later transferred to the AIPS package for calibration of the complex visibilities and imaging in a standard manner[25]. The complex visibility data have been weighted by the inverse fourth power of the signal-to-noise ratio of the complex visibility to improve the contribution of the higher spatial frequencies to the image.

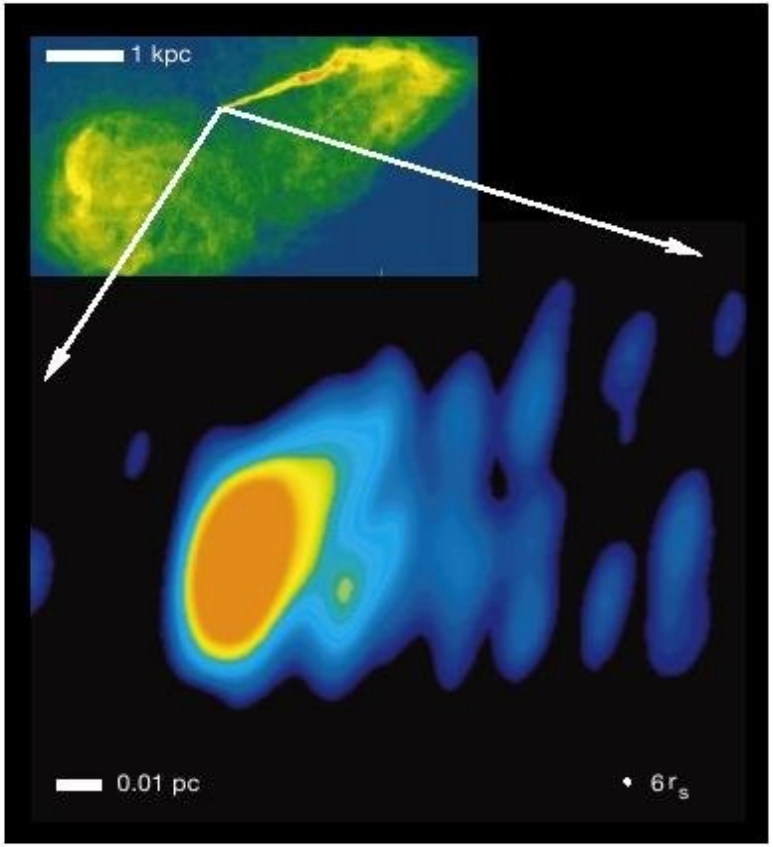

Figure 2 Pseudo-colour rendition of the nucleus of M87 at 43 GHz on 3 March 1999. See Fig. 1 for details. The filled white circle at lower right indicates $6r_S$, which is the diameter of the last stable orbit around a non-rotating black hole. The inset (top left) is a 15-GHz VLA image illustrating the large-scale jet.

3C120: Red ellipse represents inner accretion disk via Rossi XTE data, with insert showing x-ray light curve (see Marscher, 2003). Contours = 43 GHz intensity (VLBA). Inset: X-ray light curve (data courtesy of Alan Marscher and Jose-Luiz Gomez) 1 mas = 0.70 pc @ D = 120 Mpc. (see Gomez et al. 2000 Science, 289, 2317)

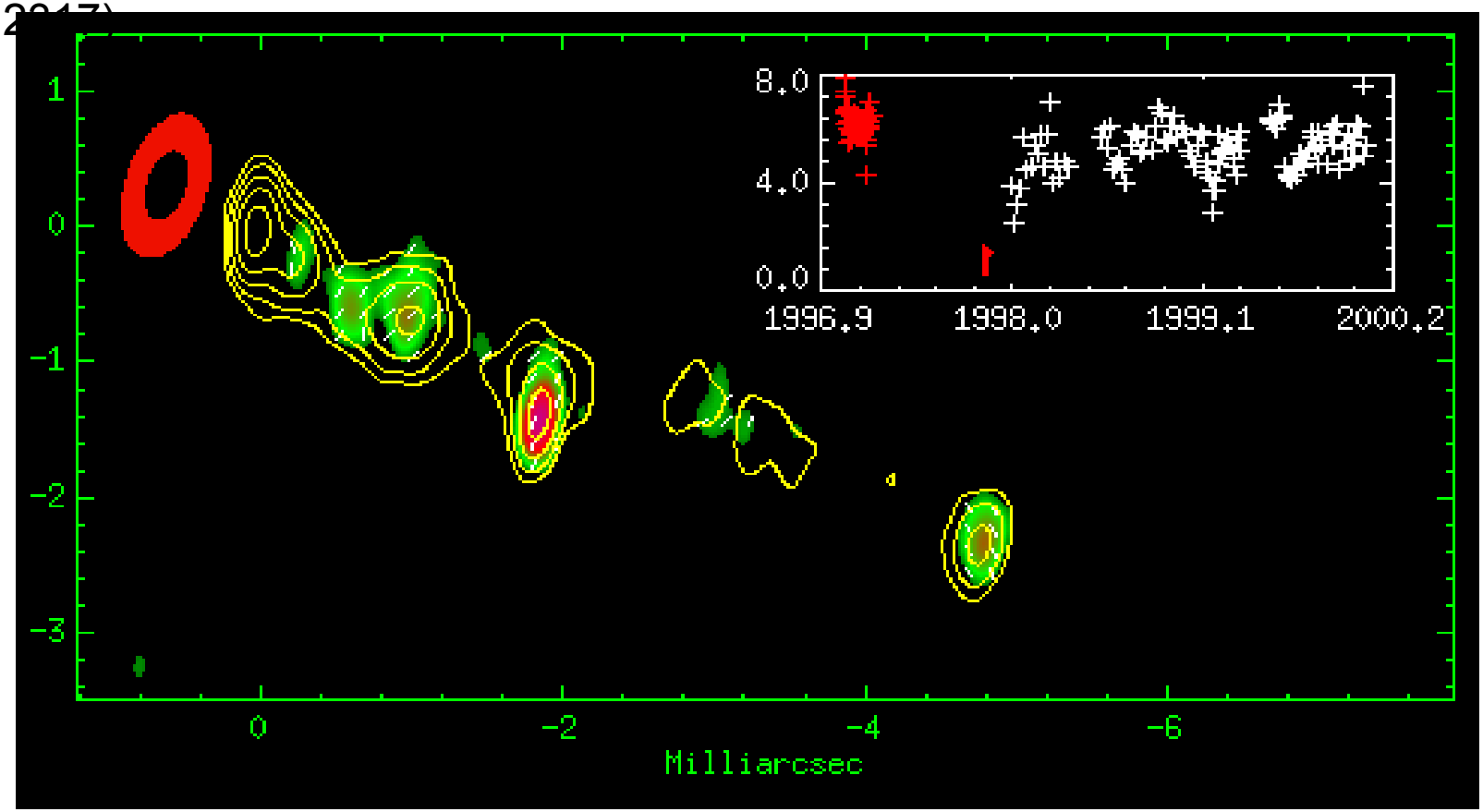

Sco X-1 frames from "movie" (see Fomalhaut, Geldzahler, and Bradshaw, 2001 Ap.J., 558, 283). For large "blobs", v = .45c. On this scale, 1 mas = 2.8 AU = 4.19×10^{13} cm with Sco X-1 at a distance, D = 2.8 Kpc (9000 light years).

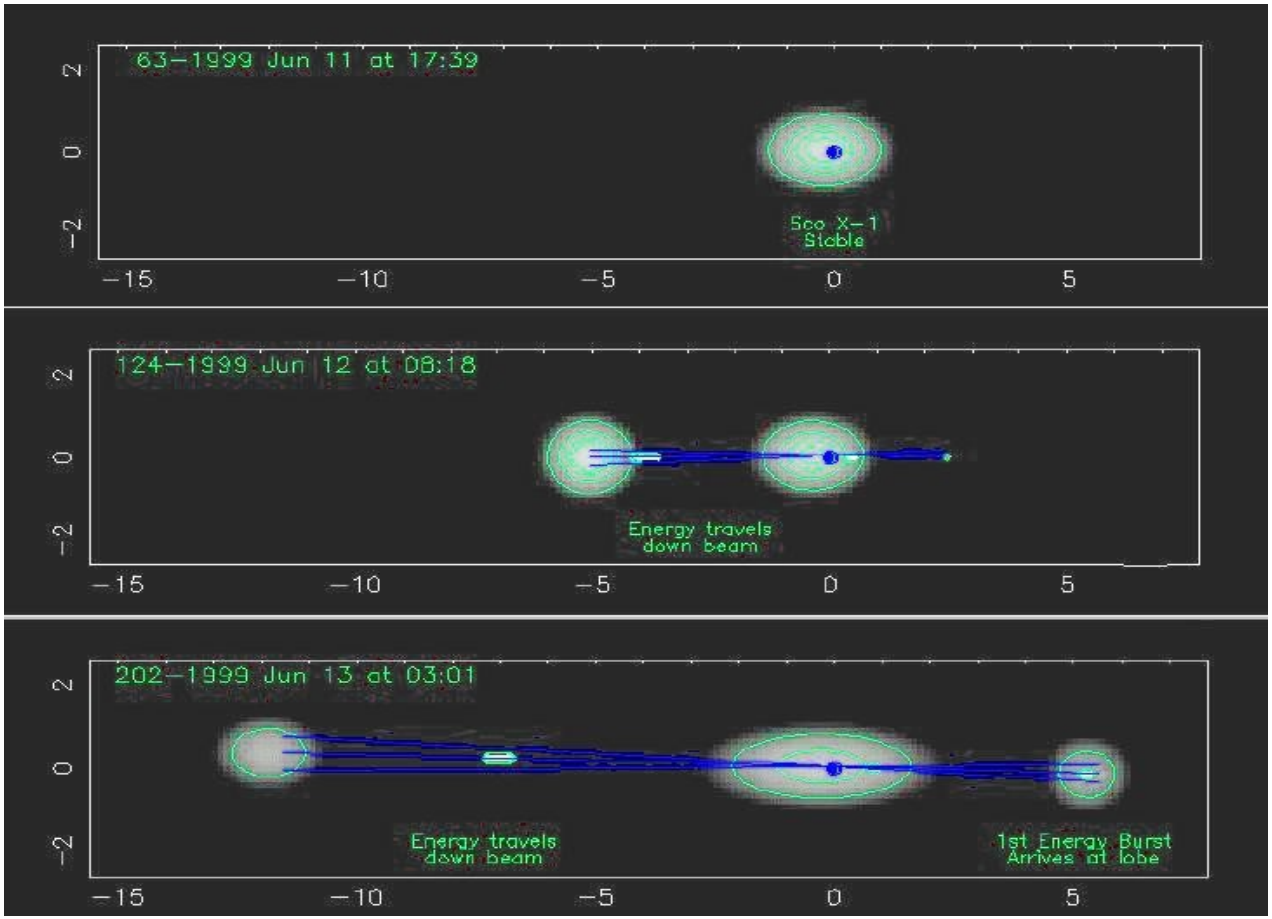

Synopsis of the work I will present (albeit briefly):

1. Energy deposition of jets into the ambient medium via plasma processes associated with caviton formation. Plasma processes are the dominant energy loss mechanism in most scenarios.

2. Momentum transfer from jet to ambient medium. We are working on article-in-cell modeling of caviton formation and dynamics in order to estimate momentum transfer from jet to ambient medium via plasma processes

3. Hydrodynamic modeling using parallelized version of VH-1 code to estimate ram-pressure momentum transfer. I will show results for a 512^3 run. We have successfully completed a 1024^3 run and are now running a 2048^3 simulation.

4. Initial results from a relativistic MHD run for an astrophysical jet using the PLUTO code (Mignone et al.). We plan to benchmark the PLUTO code by comparing its results to the VH-1 code results for a supersonic, hydrodynamic jet..

Modeling the Interaction of AGN and Microquasar Jets with the Ambient Medium:

We are developing a multi-scale code which uses the energy deposition rate and momentum transfer rate generated by a jet that generates strong plasma turbulence.

We estimate the effect of this turbulence using the LSP PIC code simulations. We then "benchmark" a code that solves a wave-population model. Ultimately we will use this wave population code to give inputs (dE/dt, dE/dx, dp/dt and dp/dx) for a highly parallelized hydrodynamic code currently running on the NRL SGI Altix.

n.b.: The wave-population code is benchmarked using a PIC (Particle-In-Cell) code in parameter ranges where a PIC code approach is feasible.

Jet-Ambient Medium Interaction

The primary energy loss mechanism for the electron-positron jet is via plasma processes:

- The two stream instability
- The oscillating two stream instability
- Ion-acoustic waves

These instabilities set up waves in the plasma which produce regions of high electric field strength and relatively low density, called “cavitons” (after “solitons” or solitary waves), which propagate like wave packets in quantum mechanics.

These mix, collapse, and reform, depositing energy into the ambient medium, transferring momentum to it, and entraining (i.e., dragging along and mixing) the ambient medium into the jet.

Jet-Ambient-Medium Interaction (continued)

In order to determine the energy deposition, momentum transfer, and heating, we model the plasma interaction as a system of coupled differential equations.

The solution to these equations gives a normalized wave energy. This wave energy density is then used to determine:

- the energy deposition rate of the jet into the ambient medium,
- the propagation length,
- the heating of the ambient plasma, and
- the momentum transfer rate.

For hadronic (p, e+/e-, etc.) the energy extracted by plasma processes slows the e+/e- component first. When the jet e+/e- component slows, the hadrons drag the along e+/e- component. The hadrons thus provide the inertia and energy transport necessary to produce the extended jets.

Two-stream instability growth rate for a cold beam:

$$\Gamma_1 = \mathrm{Im}\,\omega \approx \frac{3^{1/2}}{2\gamma}\left(\frac{n_b}{2n_p}\right)^{1/3}\omega_p$$

Two-stream instability growth rate for a warm beam:

$$\Gamma_1 = \mathrm{Im}\,\omega \approx \frac{1}{\gamma}\frac{n_b}{n_p}\frac{1}{(\Delta\theta)^2}$$

Landau damping for plasma waves in a two-temperature gas

$$\frac{\Gamma_{LD}}{\omega_p} = g_L = \sqrt{\frac{\pi}{8}} K^{-3} \left[(1 - f_h) \exp\left(-\frac{1}{2} \left(K^{-2} + 3b \right) \right) + f_h \left(\frac{T_c}{T_h} \right)^{3/2} \exp\left(-\frac{T_c}{2T_h} (K^{-2} + 3b) \right) \right],$$

where $K = \kappa_2 \lambda_D$, T_c is the cold temperature and T_h are the hot temperatures for gas, $f = n_h/(n_c+n_h)$; n_c and n_h are the cold and hot number densities of the gas, and $b = 1-f_h+T_h/T_c)$, and f_c and f_h are the cold and hot fractions of the gas.

Wave Population Rate Equations: a system of coupled, differential equations that model the plasma interactions with the ISM/ICM

$$\frac{\partial W_1}{\partial t} = \left[2\Gamma_1 W_1 H\left(\frac{\epsilon_w}{n_p T_e} - W_1\right)\right] - \left[2\Gamma^{DO}(W_s)W_1 + 2\Gamma^{OTS}(W_1)W_2 H(W_1 - k_1^2\lambda_D^2)\right]$$

$$\frac{\partial W_2}{\partial t} = \left[2\Gamma^{DO}(W_s)W_1 + 2\Gamma^{OTS}(W_1)W_2 H(W_1 - k_1^2\lambda_D^2)\right]$$

$$- \left[2\Gamma_L W_2 + 2\Gamma^{OTS}(W_2)W_s H\left(W_2 - \frac{4}{\omega_p}\Gamma_L\right) + \frac{W_2}{\tau_2}\right],$$

$$\frac{\partial W_s}{\partial t} = \left[2\Gamma^{OTS}(W_1)W_s H(W_1 - k_1^2\lambda_D^2) + 2\Gamma^{OTS}(W_2)W_s H\left(W_2 - \frac{4}{\omega_p}\Gamma_L\right)\right]$$

The plasma wave interactions are similar to a predator-prey system

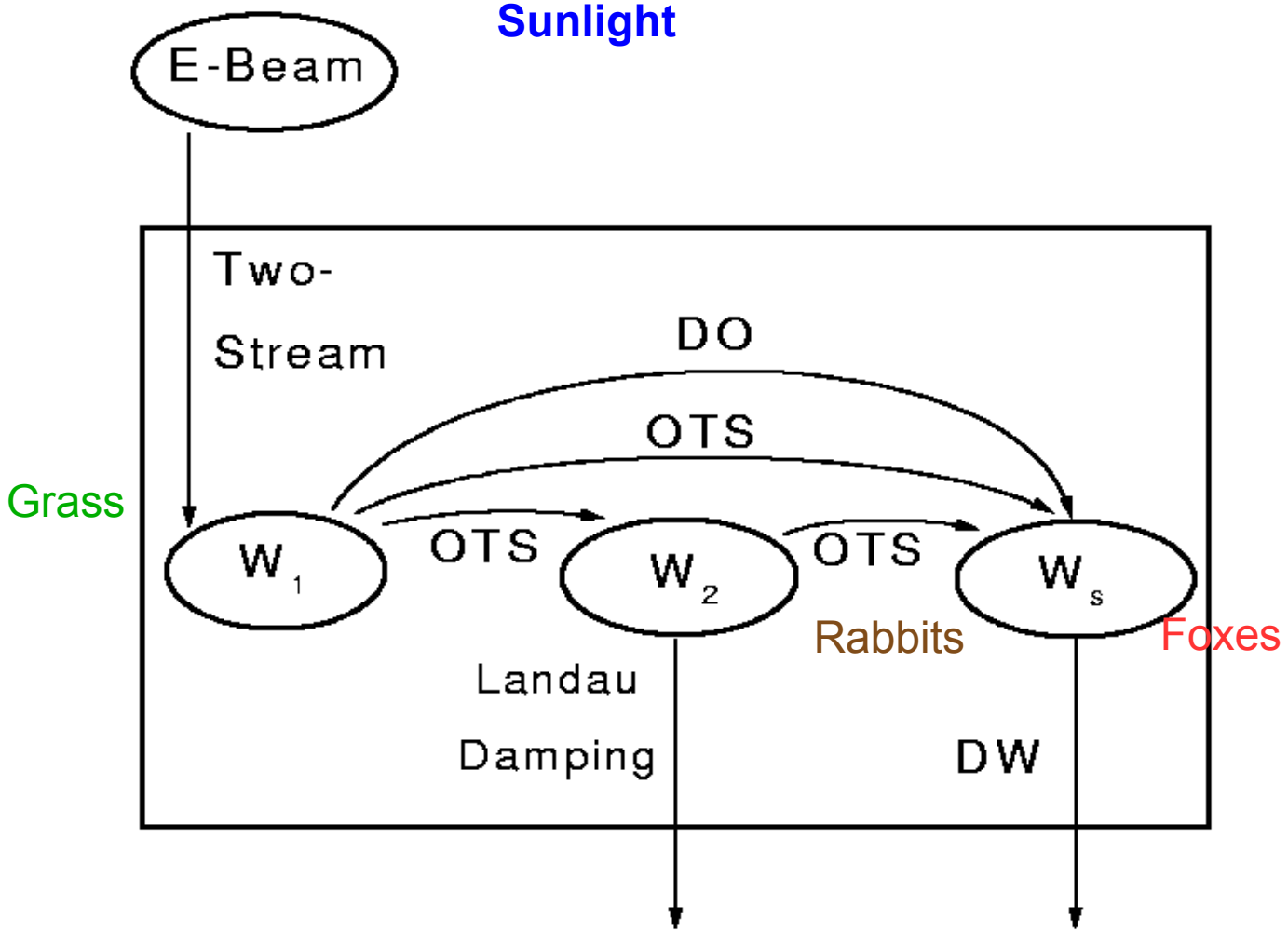

The environment that the jets propagate through is very complex.

The range of densities involved in the interaction varies over many orders of magnitude, and the jet itself clearly evolves by a number of mechanisms:

- Energy loss by various loss mechanisms*
- Entrainment of the ambient medium contributes to the changes in the jets' constitution through losses and acceleration of particles.

(*see, e.g., Scott Holman, Ionson, and Papadopoulos, 1980 Ap.J. 239, 769, Rose, Guillory, Beall, and Kainer, 1984 Ap.J., 280, 550; and Beall 1980 in *Physical Processes in Hot Cosmic Plasmas*, Kluwer Pub.).

Typical solutions to the wave population equation can be damped, oscillatory, or chaotic, depending on jet and ambient medium parameters.

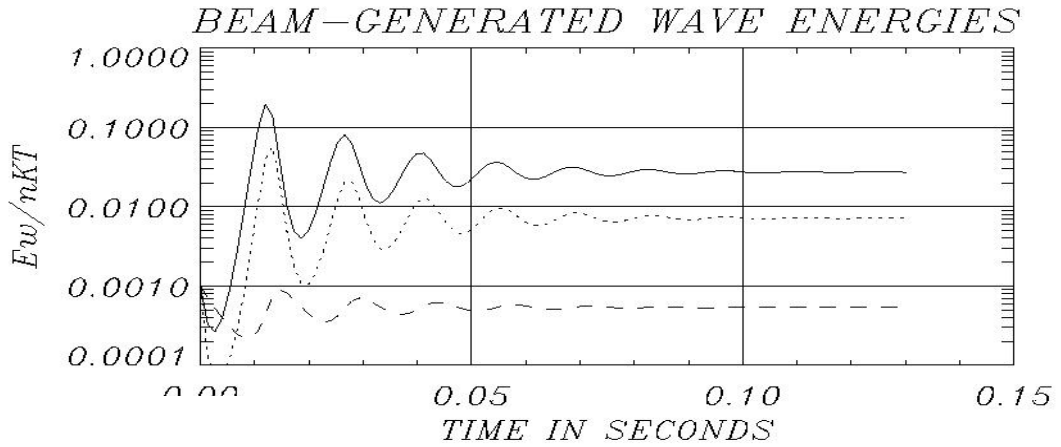

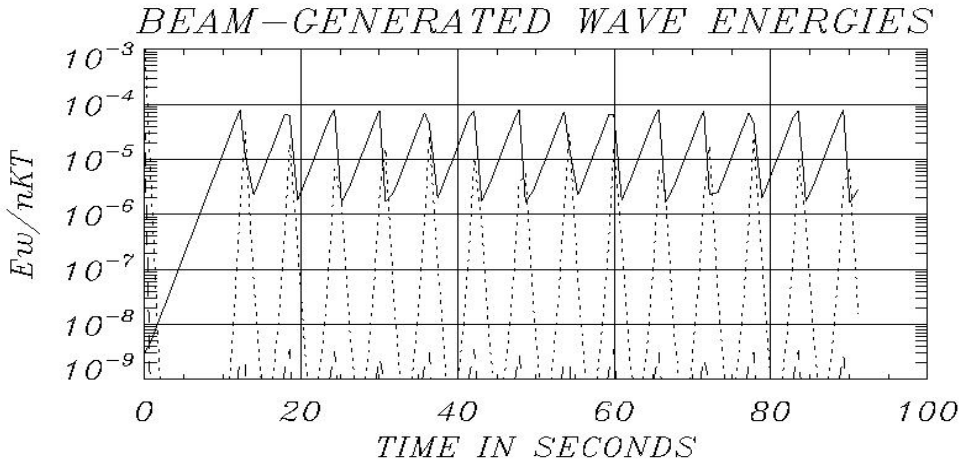

Energy Deposition Rate of Jet Energy Into Ambient Medium

The average energy deposition rate is given by the average normalized wave energy, W, as follows:

$$dE/dt = \langle d\alpha\varepsilon/dt \rangle = nkT \langle W \rangle \Gamma_1 \text{ ergs cm}^{-3}\text{s}^{-1}$$

where n is number density of the ambient medium, <W> is the average normalized wave energy density obtained from the wave population code, and Γ_1 is the growth rate of the two-stream instability.

Collisionless (Plasma) Losses:

$$dE_{plasma}/dx = -(1/n_b v_b)(d\alpha\epsilon_1/dt),$$

can be obtained by determining the change in γ of a factor of 2 with the integration:

$$\int d\gamma = -\int [d(\alpha\epsilon_1)/dt]/(v_b n_b m^{'} c^2)$$

as shown in Rose et al., 1978 and Beall 1990. Thus,

$$L_p = ((1/2)\gamma c n_b m c^2)/(d\alpha\epsilon_1/dt)$$

is the characteristic propagation length for collisionless losses for an electron or electron-positron jet. In many astrophysical cases, this is the dominant energy loss mechanism.

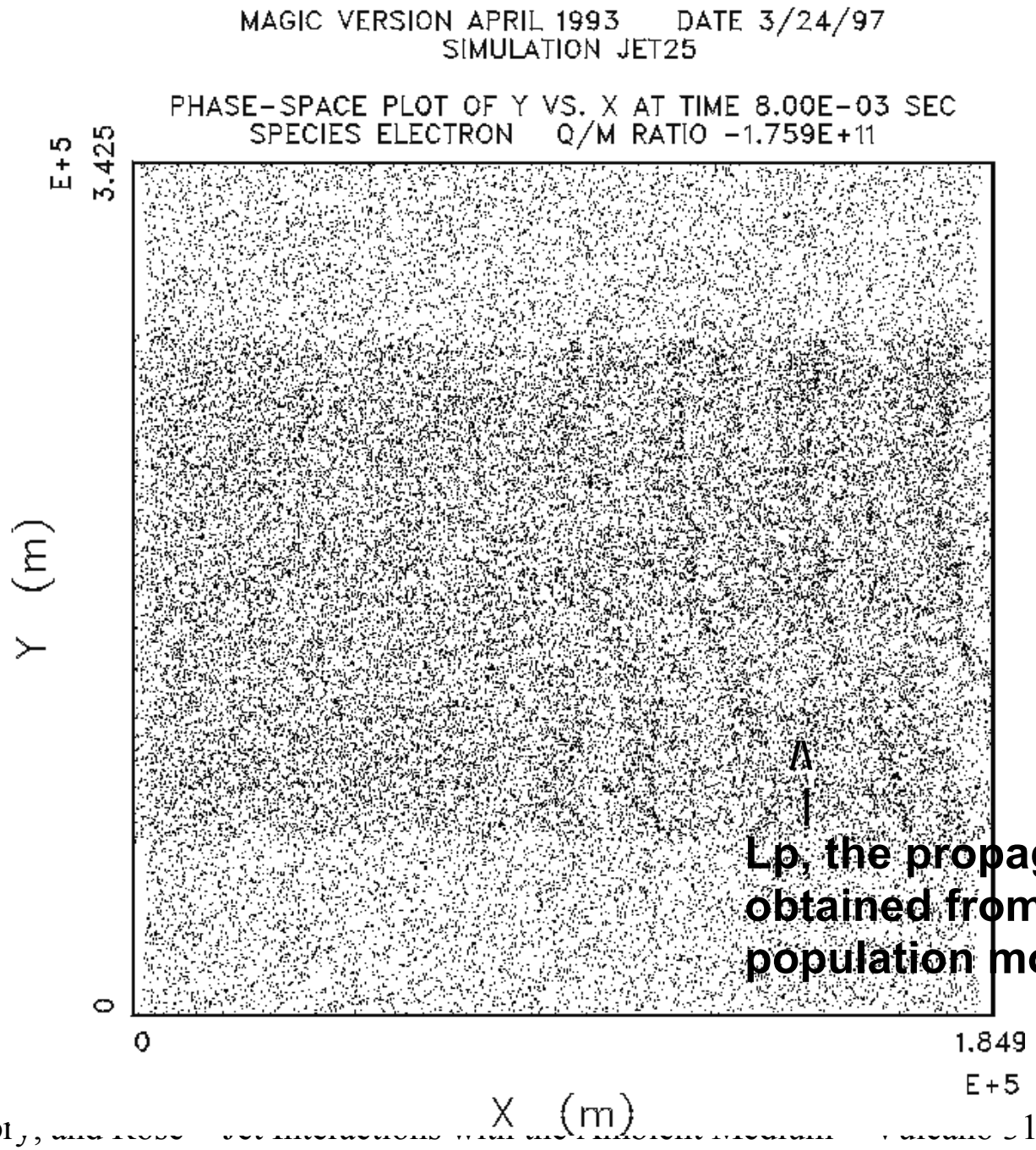
MAGIC VERSION APRIL 1993 DATE 3/24/97
SIMULATION JET25
PHASE-SPACE PLOT OF Y VS. X AT TIME 8.00E-03 SEC
SPECIES ELECTRON Q/M RATIO -1.759E+11
E+5
3.425
Y (m)
0
0
1.849
E+5
X (m)
Λ
|
Lp, the propagation length obtained from the wave population model code

Jet25 – γ=2 electron-positron beams, $n_p/n_b = 20$, $B_x \sim 4B_c$

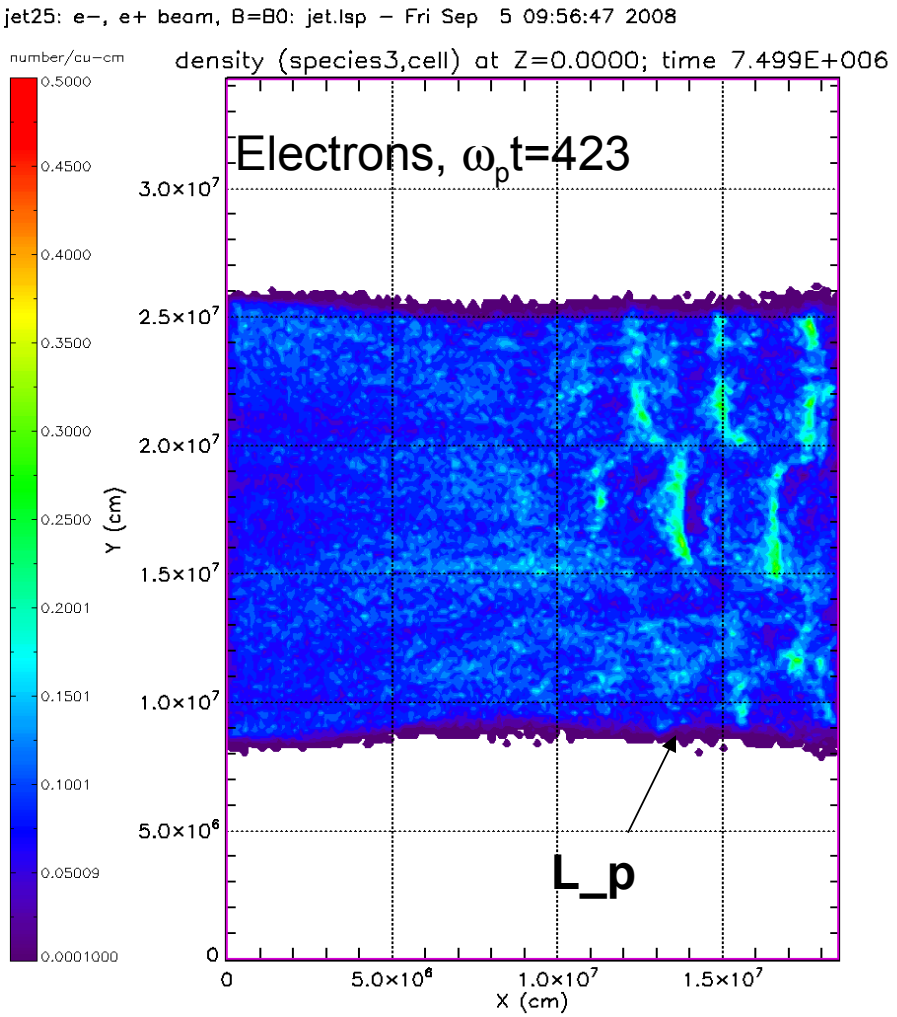

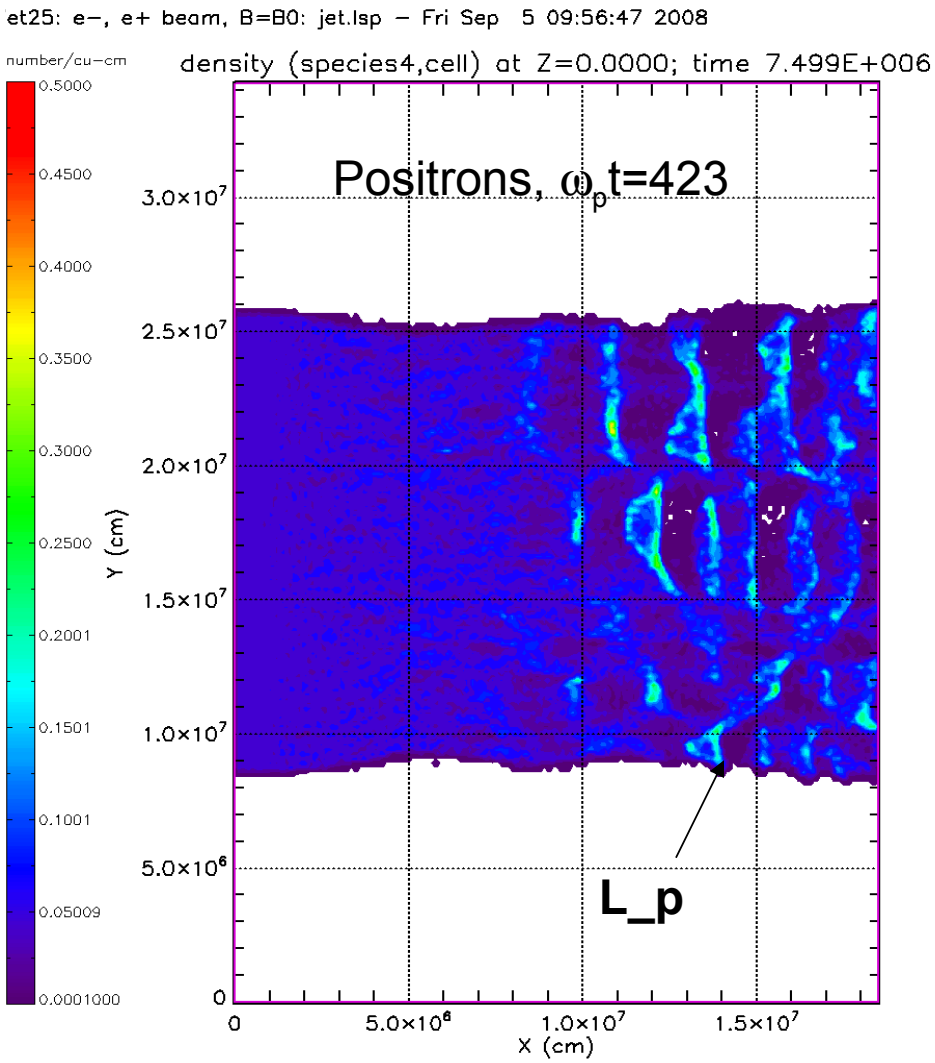

Beall, Guillory, and Rose – Jet Interactions with the

Collapse of soliton or "caviton" generated
by a jet propagating through an ambient medium.

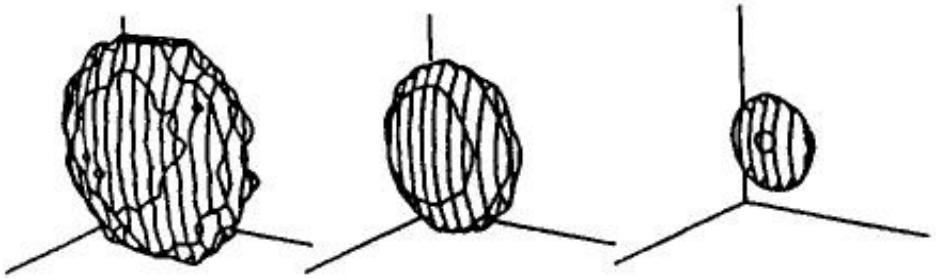

FIG. 1. Collapse of a three-dimensional Langmuir wave packet seen in numerical simulations (Robinson *et al.*, 1988). A surface of constant electric-field strength is drawn at 80% of the maximum value at the center of the packet. Time increases to the right and each frame has linear dimensions of 80 Debye lengths [see Eq. (2.1) for definition] in each direction.

Rev. Mod. Phys., Vol. 69, No. 2, April 1997

$$\lambda_D = (kT/4\pi ne^2)^{1/2} = 7.43 \times 10^2 (T/n_p)^{1/2} \text{ cm.}$$

$$\omega_p = (4\pi ne^2/m)^{1/2} \text{ , and } 2\pi f_p(\text{in Hz}) = \omega_p$$

Heating the Ambient Medium via Non-thermal Electron Tails: Evolution Examined Theoretically

To estimate the work done on background electrons entering the caviton, we note that:

$$de/dt = \int J \cdot E \, dV$$

where J is the current density, E is the time-averaged electrit field within the caviton, and dV is the differential volume of the caviton. We estimate the current density as:

$$J = 2q \int v \, f_e(v) dv$$

Where q is the charge, v is the velocity with limits v_{th} to infinity, $f_e(v)$ is the distribution function, and we are interested in electrons entering the cavity from both directions.

Non-thermal Electron Tails in the Maxwell-Boltzmann Distribution: Evolution Examined Theoretically

$J = 2q \int v\, f_e(v) dv$ thus has the form of an integral $\int x\, e^{-x\hat{}2} dx =$ 1/2e, from 1 to infinity, where we have ignored the effect of the potential of the caviton on the distribution function.

The volume of the caviton = $(\alpha\lambda_D)^3$, and the caviton density is equal to the normalized wave energy density. Therefore,

$$de/dt = 2.7 \times 10^{-7}\ \alpha^3\ T^4\ W_1/n_e^{3/2}\ \text{ergs/cm}^3\text{s}$$

This energy deposition rate can power the BLR in a typical AGN from the two-stream instability processes.

Non-thermal electron tail evolution: examined in PIC code simulations

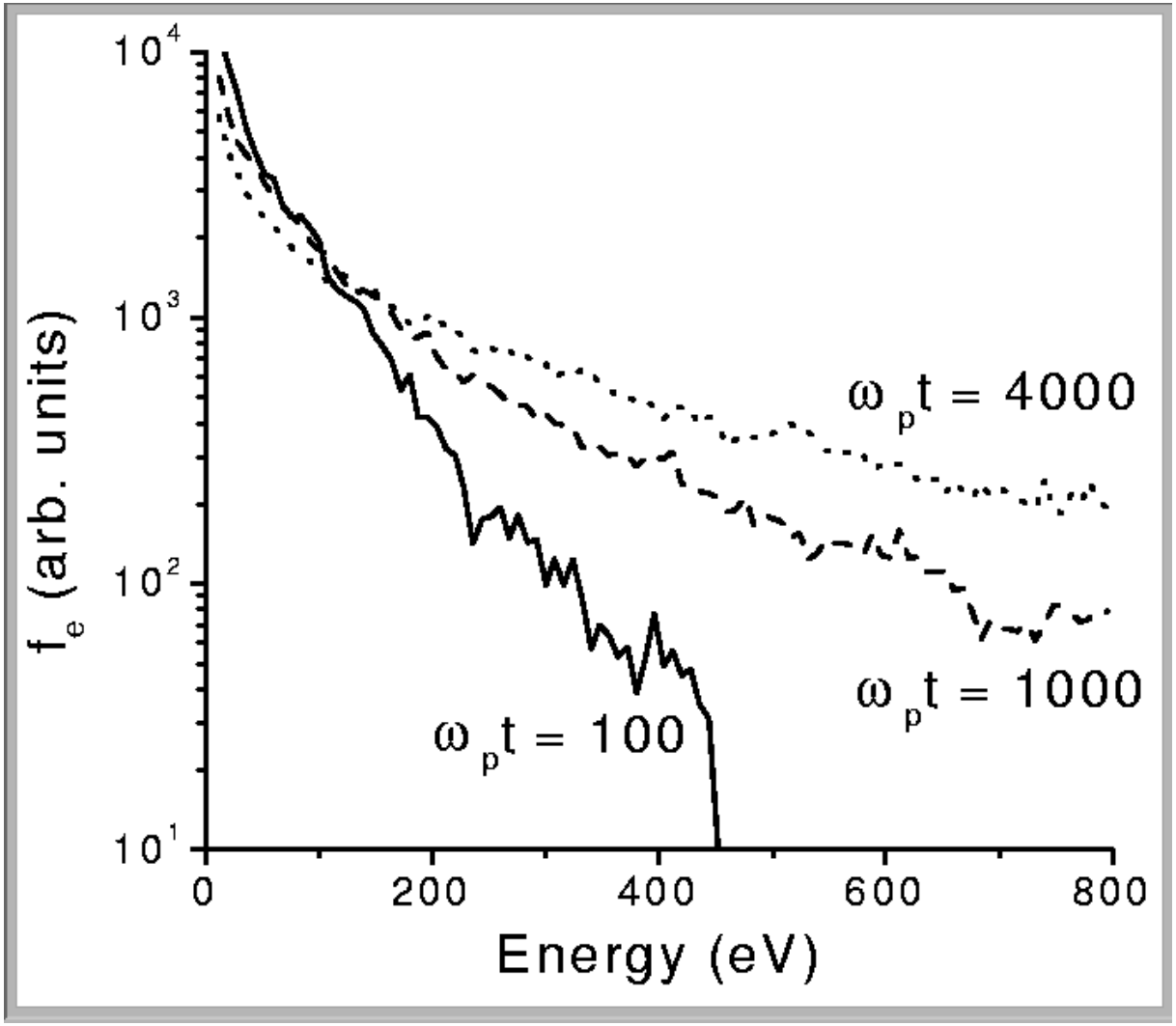

- Simulations track the evolution of the electron and ion distributions for an electron beam propagation in a dense (R=0.01) background plasma, where $R=n_b/n_p$

Shock Heating

If we consider the effect on heating from strong shocks, the classical result is:

$$\rho_2/\rho_1 = (\gamma+1)/(\gamma\ -1) \sim 4/1,$$

where the polytropic index, $\gamma = 5/3$, for a monatomic, ideal gas.

(see e.g., Manami Sasaki's talk on Wednesday)

Since the temperature for an ideal gas follows the density (assuming constant pressure), the temperature differential due to shock heating is $T_2/T_1 \sim 4/1$.

Note that the estimates of heating of the gas due to plasma processes is roughly $T_2/T_1 = 10^5\text{K}/10^4\text{K}$. i.e., an order of magnitude greater than shock heating..

Strong Turbulence and the Collapse of Wave Packets

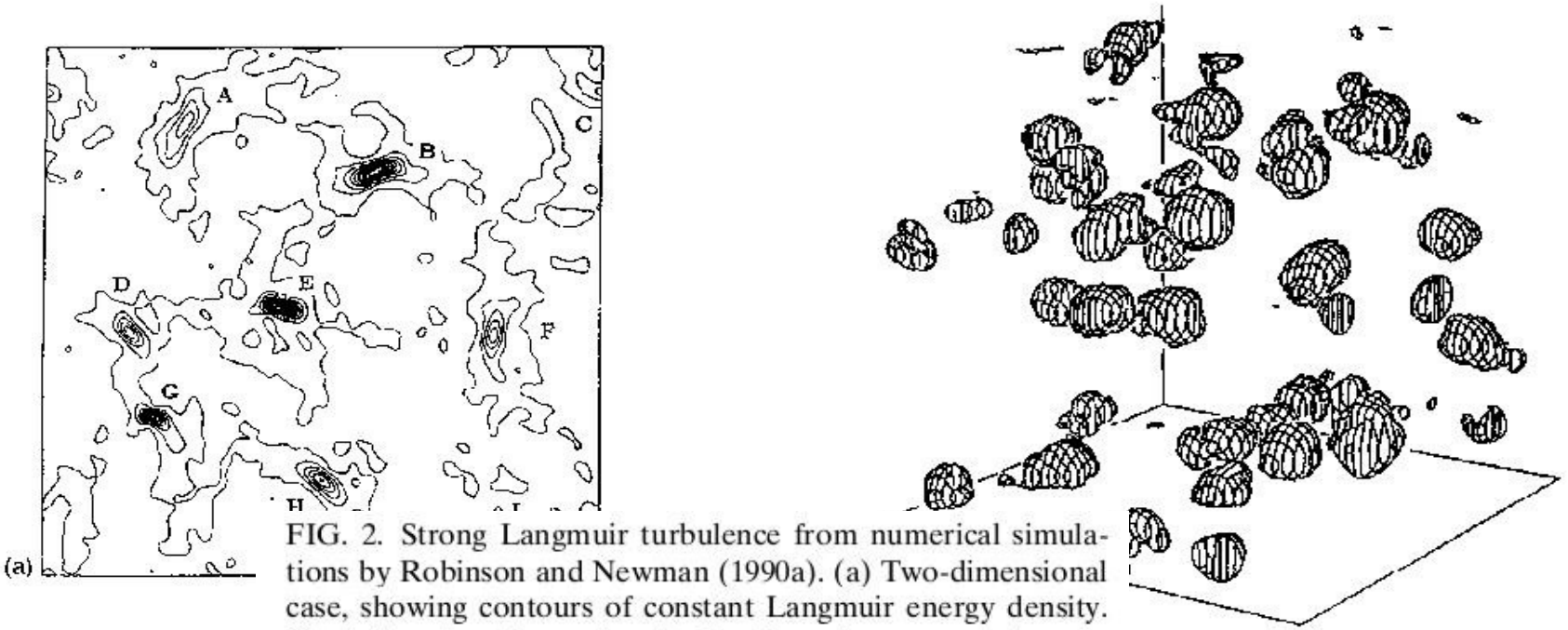

FIG. 2. Strong Langmuir turbulence from numerical simulations by Robinson and Newman (1990a). (a) Two-dimensional case, showing contours of constant Langmuir energy density. The lettered peaks are localized, coherent wave packets, subject to collapse. Regions in between are filled with low-level incoherent waves. The system has dimensions of 1340 Debye lengths [see Eq. (2.1) for definition] in each direction. (b) Three-dimensional case, showing a surface of constant energy density at 10% of the maximum value, enclosing the high-field regions of localized, coherent wave packets. Regions in between are filled with low-level incoherent waves. The system has dimensions of 800 Debye lengths in each direction.

We have confirmed the Newman *et al*. (Newman:1990) 2D PIC collapse simulations.

- 2D PIC simulations were compared directly with 2D Zakharov equation model.
- 2D PIC simulations used an ion density "depression" to drive Langmuir wave packets.
  - Despite relatively modest spatial and particle resolutions, good agreement between the two models was obtained.
- Below, we describe LSP simulations that mimic the basic simulation model presented in [Newman:1990].

Case with a 5.5% density depression:

- The initial fields closely resemble the example given in Fig 1(b) of [Newman:1990]:

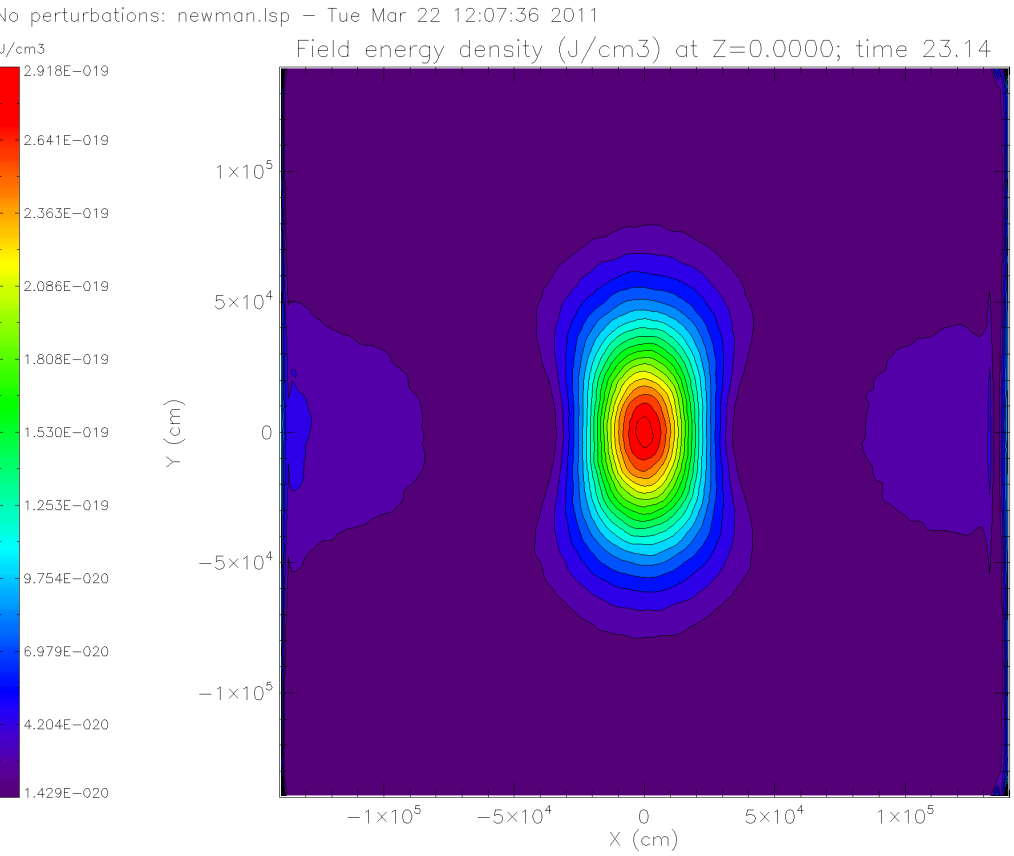

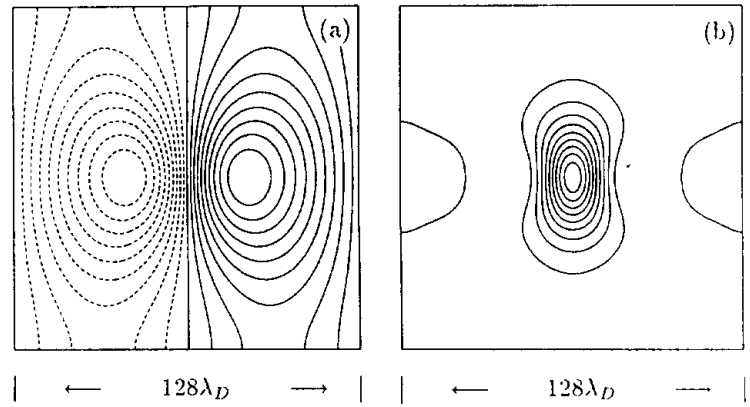

FIG. 1. Initial Langmuir field. (a) Contours of constant Re ϕ at intervals of 10% of the maximum. (b) Contours of constant $|\mathbf{E}|^2$ at intervals of 10% of the maximum. Dashed lines represent negative values.

Newman05-ES: uniform ion density (perturbation applied to electrons)

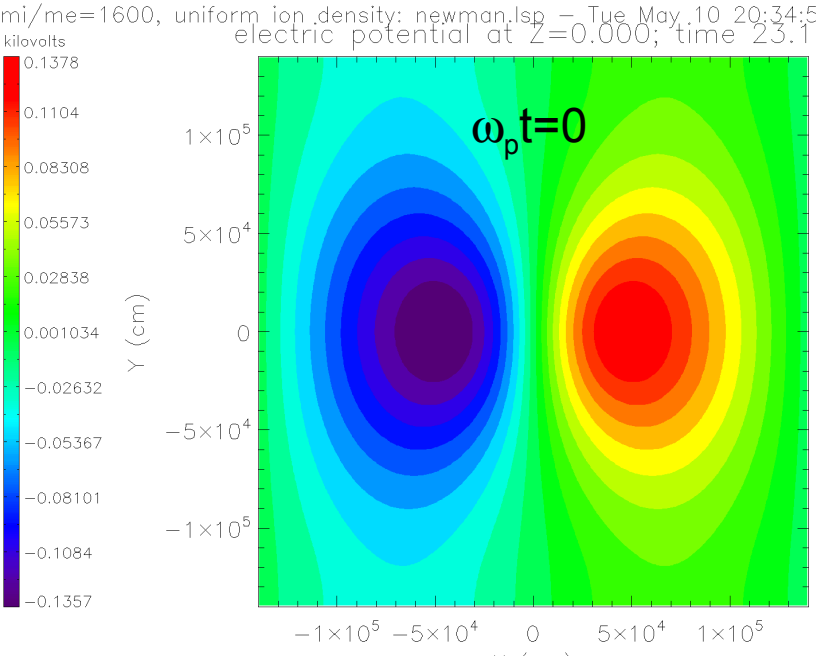

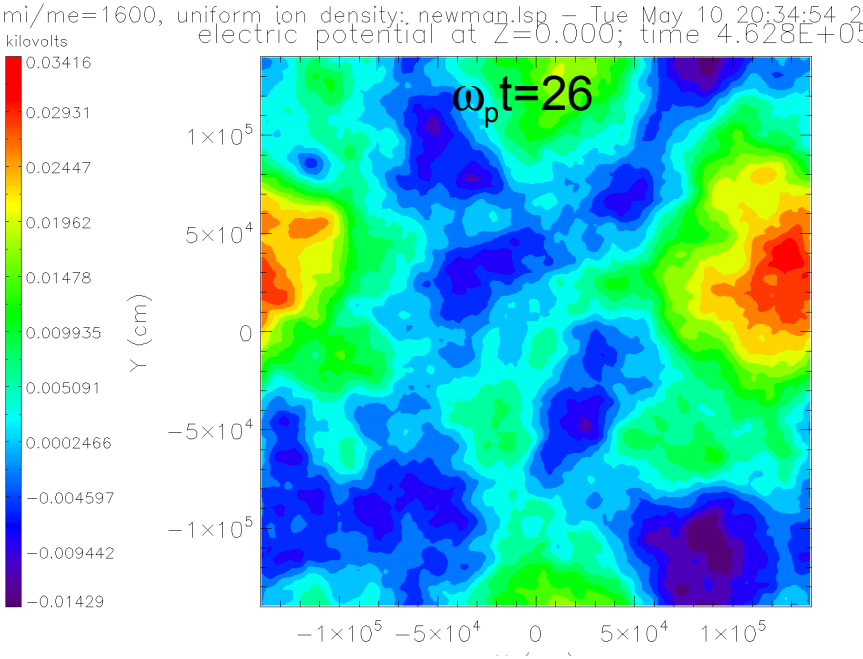

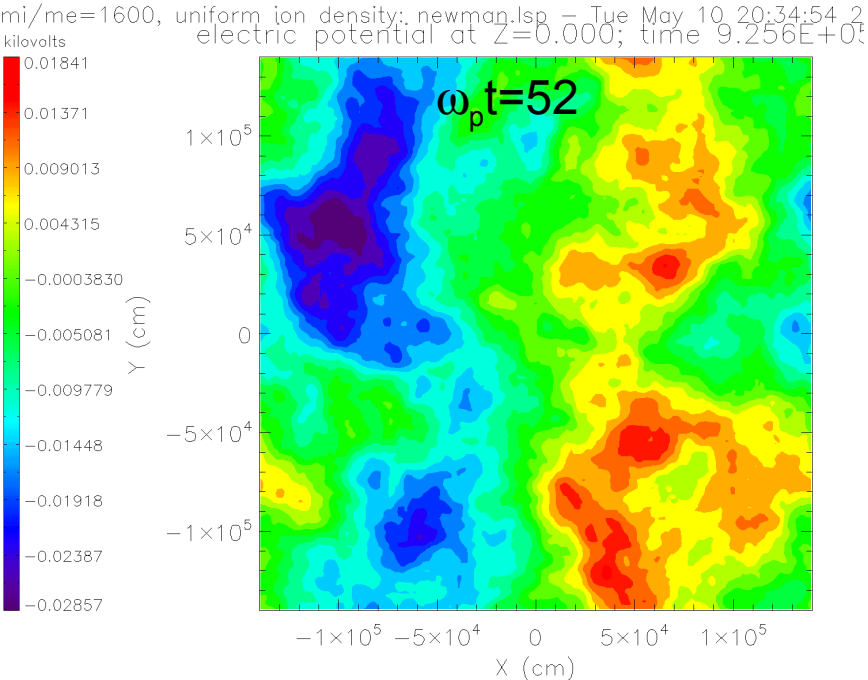

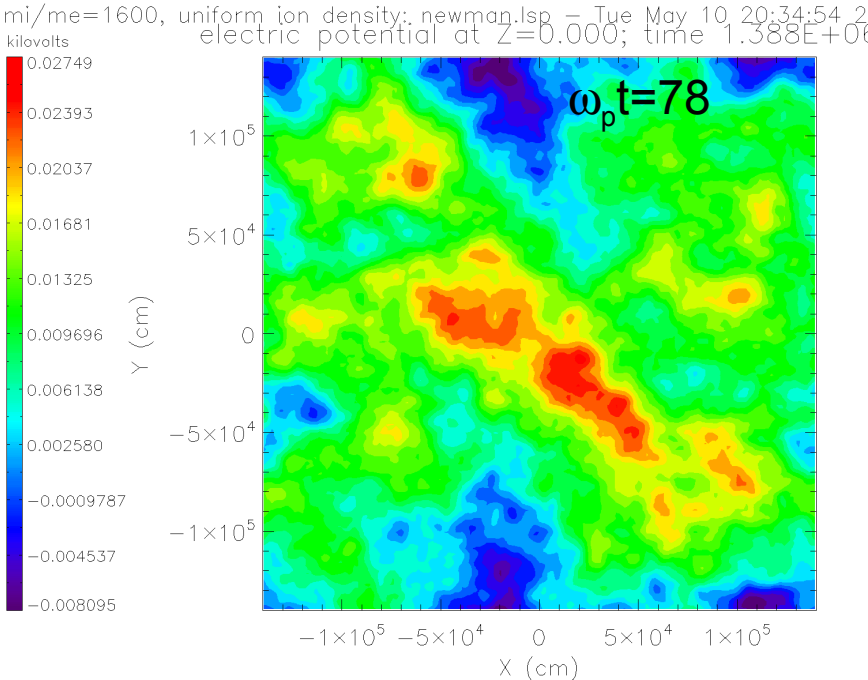

Newman05-ES: uniform ion density (perturbation applied to electrons)

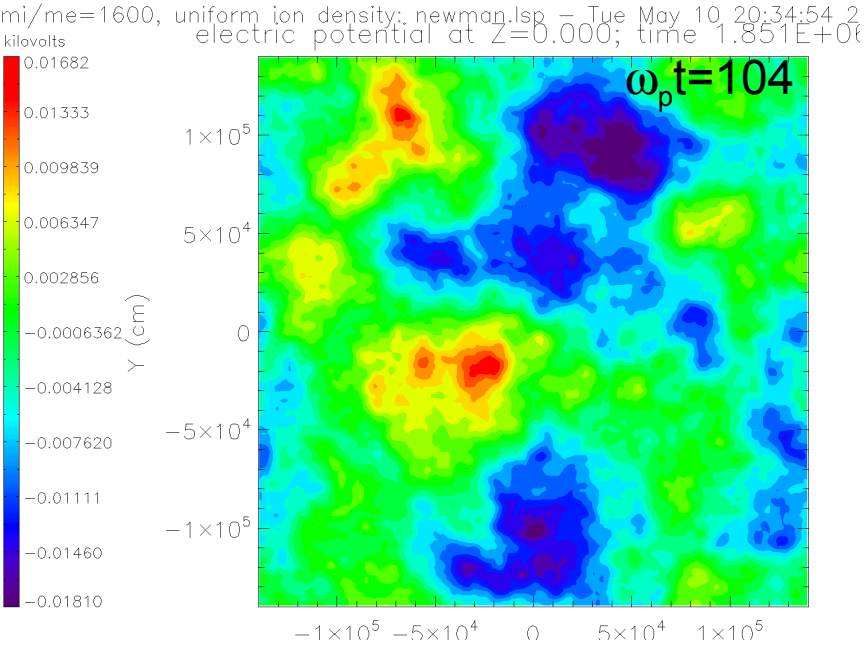

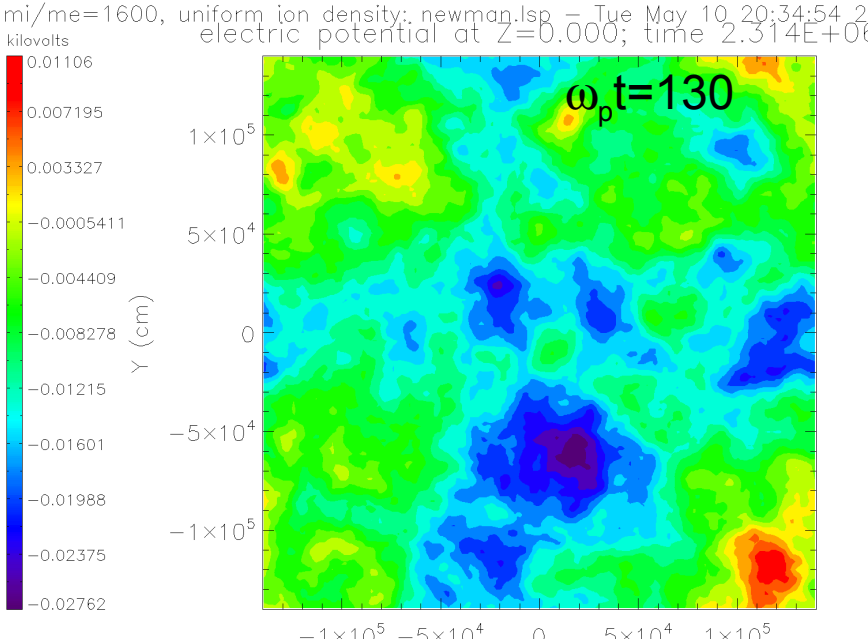

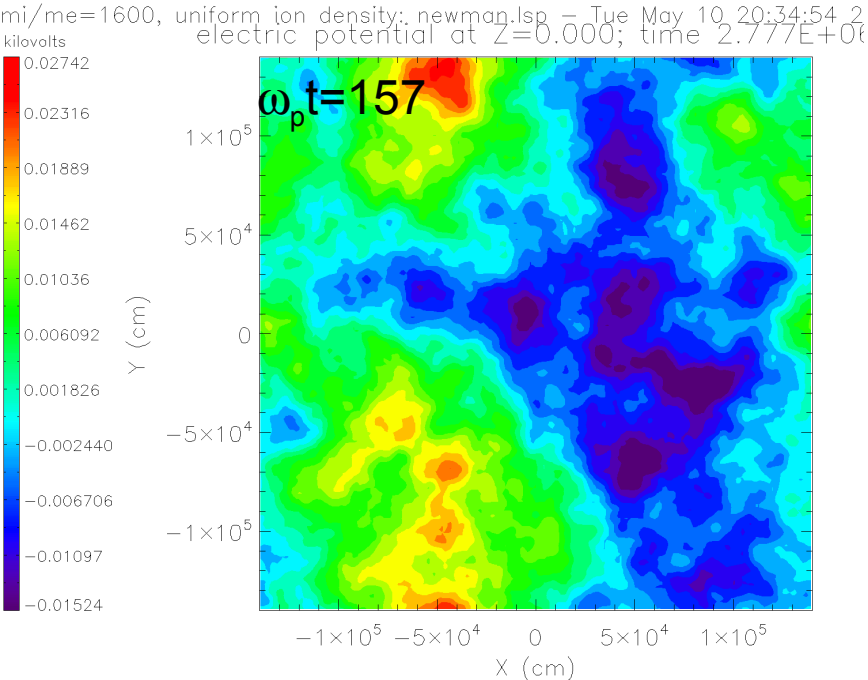

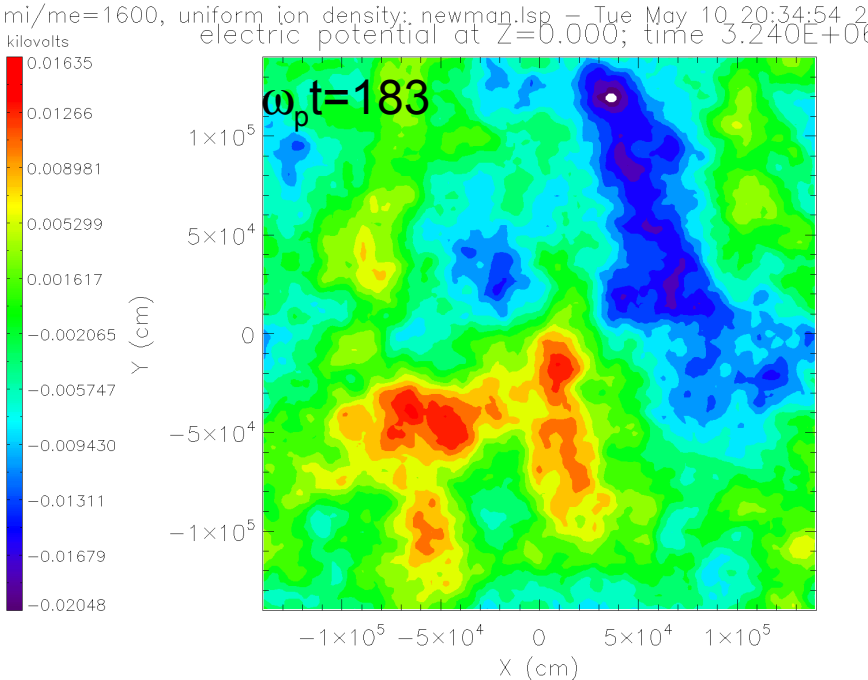

PIC code caviton formation illustrates net positive axial momentum of density structure:

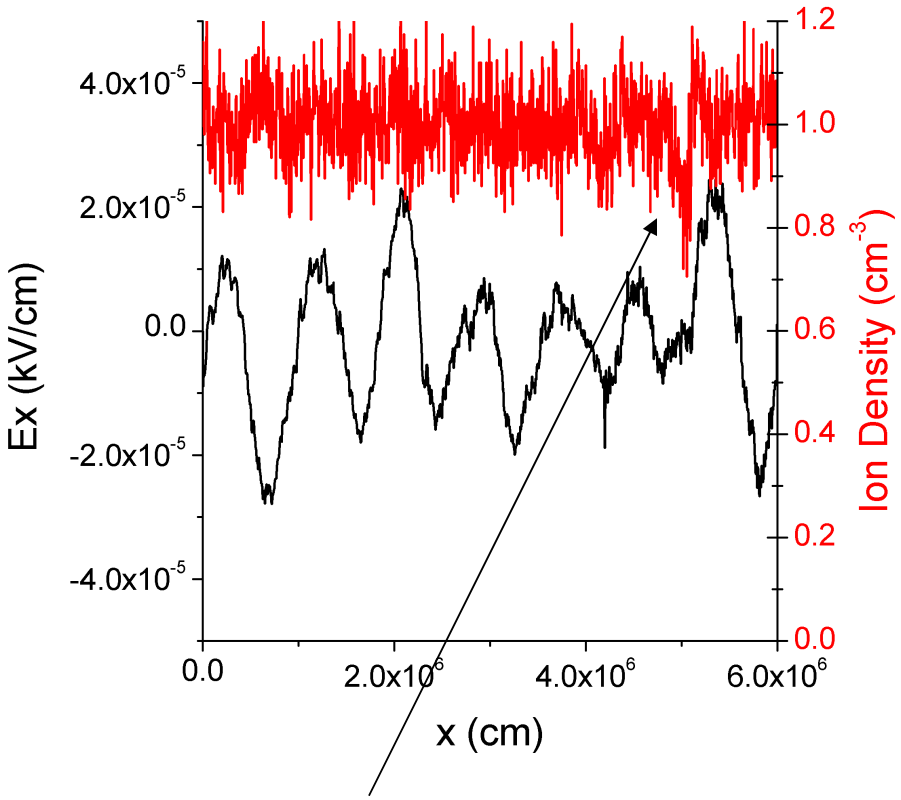

Sample caviton:

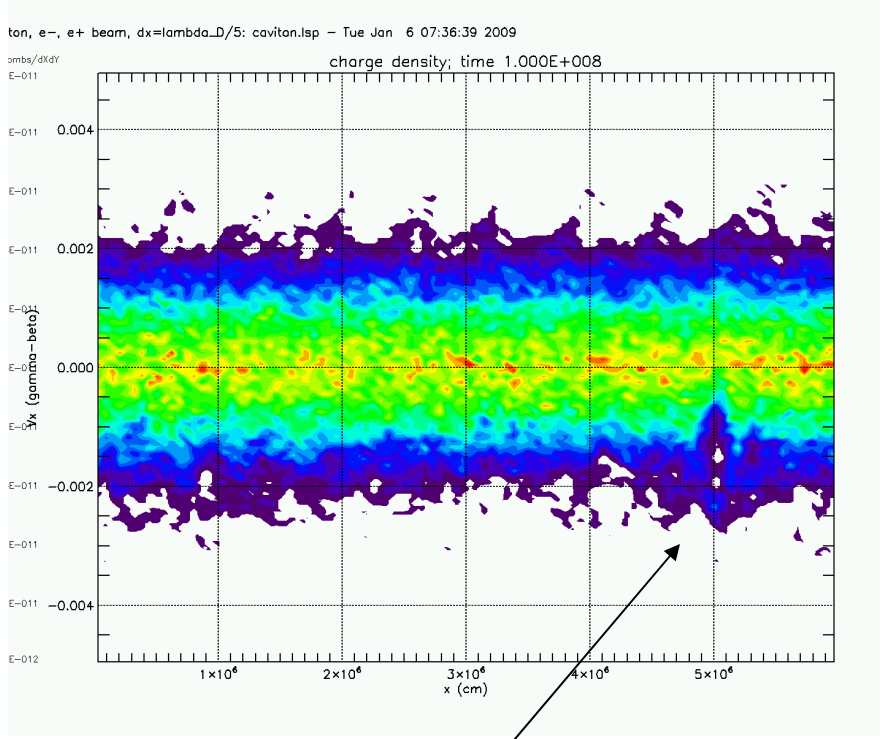

Ion phase space contours show that caviton has a net forward directed momentum:

3. Simulation of AGN jet using highly parallelized version of VH-1 hydrodynamic code

$$\partial_t \rho + \nabla \cdot (\rho \mathbf{u}) = 0,$$
$$\partial_t (\rho \mathbf{u}) + \nabla \cdot (\rho \mathbf{u}\mathbf{u}) + \nabla p = \mathbf{F},$$
$$\partial_t (\rho \mathcal{E}) + \nabla \cdot (\rho \mathcal{E} \mathbf{u}) + \nabla (p \mathbf{u}) = G + \rho \mathbf{u} \cdot \mathbf{F},$$

n.b.: Code yields estimates of temperature, density, velocity (v_x,v_y and v_z), and cooling rate for each volume in the simulation.

The highly parallelized VH-1 code is running on the NRL SGI Altix supercomputer. Kinwah Wu and Curtis Saxton (MSSL, UK) are collaborators on this part of the project.

VH-1 Simulation of a Supersonic Jet

512^3 shown. 1024^3 finished. 2048^3 run is underway (estimated to take 150,000+ CPU hrs.

Figure 1 below shows the x-z coss-section of the pressure of the ambient medium and jet (along the central axis) for a jet with **v = 1.5e9 cm/sec.**

The data from Figures 1 and 2 can be combined to show the areas of jet-induced star formation.

Figure 2 below shows the x-y cross-section of the density structures of the same jet and ambient medium.. The simulations shown are from the analysis of the 512^3 runs. The length of the jet is 64 kpc.

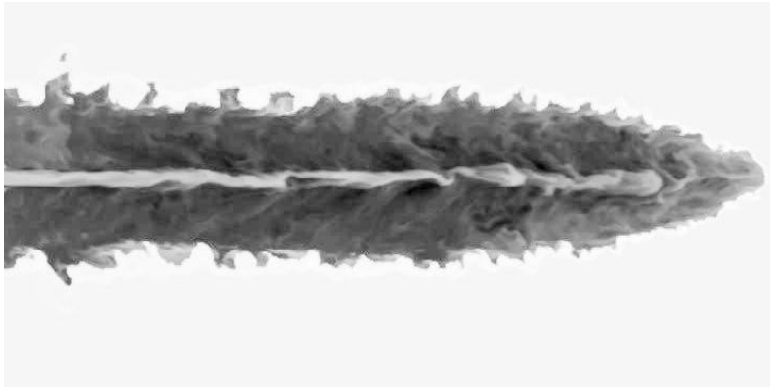

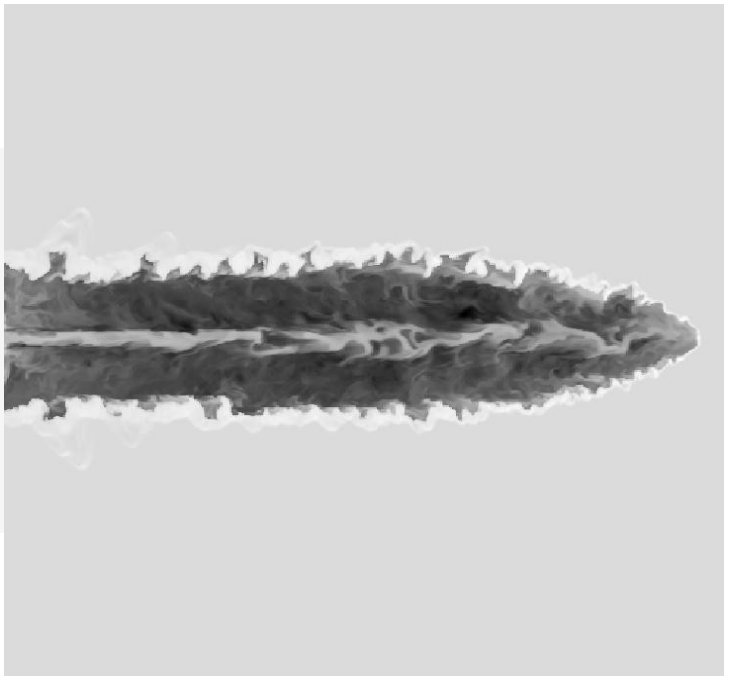

Figure 3 below shows the x-z coss-section of the density of the ambient medium and jet (along the central axis) for a jet with **v = 1.0e9 cm/sec**.

Figure 4 below shows Jeans Length relative Jeans Length for the same jet in the x-z cross-section. The simulations shown are from the analysis of the 512^3 runs. The length of the jet is 64 kpc.

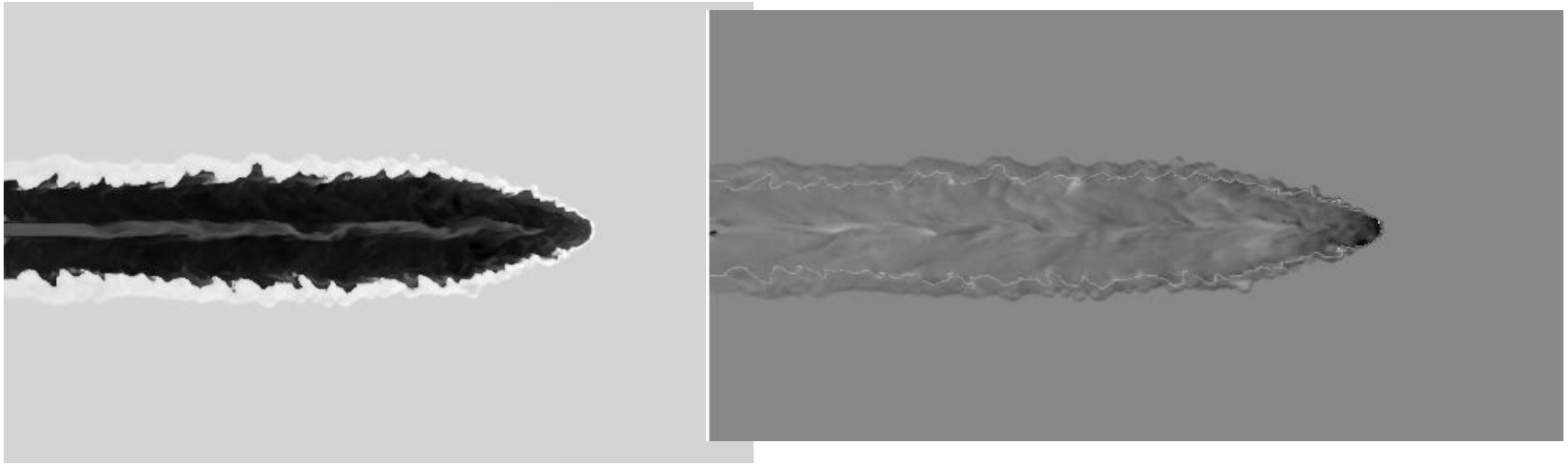

Parallelized VH-1 Large-Scale Jet Simulation shown with a volumetric rendering

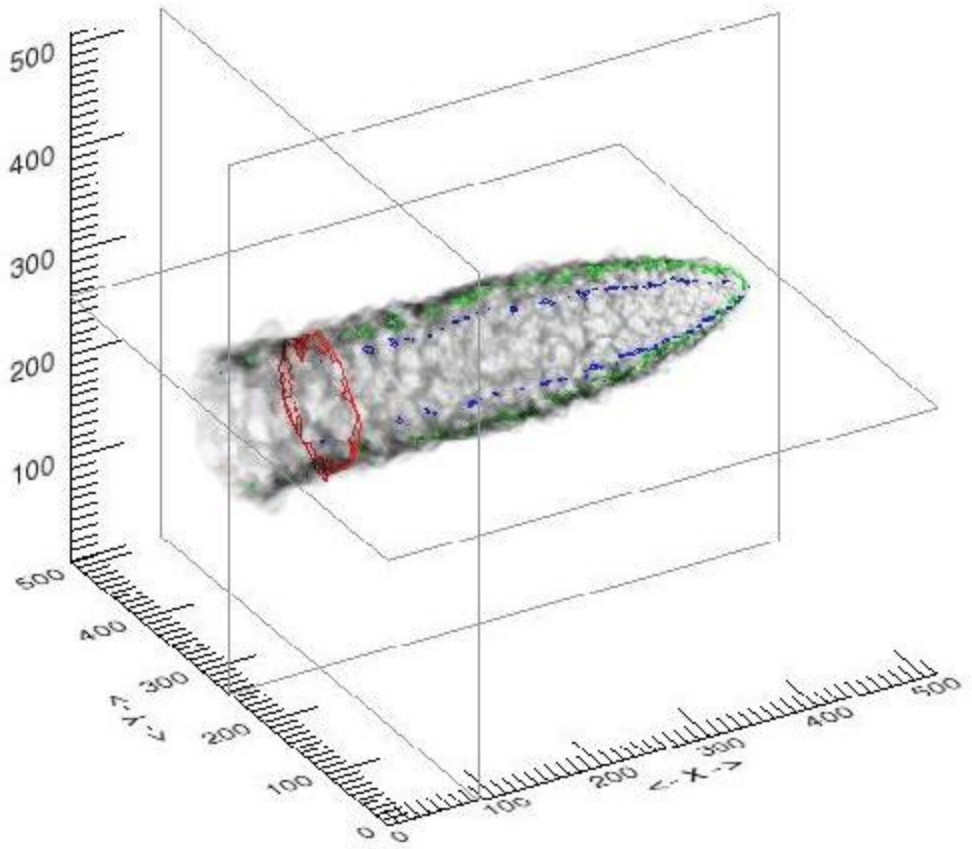

Volumetric rendering of relative intensity of star formation rates (via Jeans' length estimates) derived from Figures 1 and 2 (fast jet) and Figures 3 and 4 (slow jet) on previous slides. The region shown is in the central section of the jet. Figure are to the same scale (indicating the fast jet has a larger effect). Scale of the images of of order 5 Kpc.

Fast Jet (v=1.5e9 cm/s)

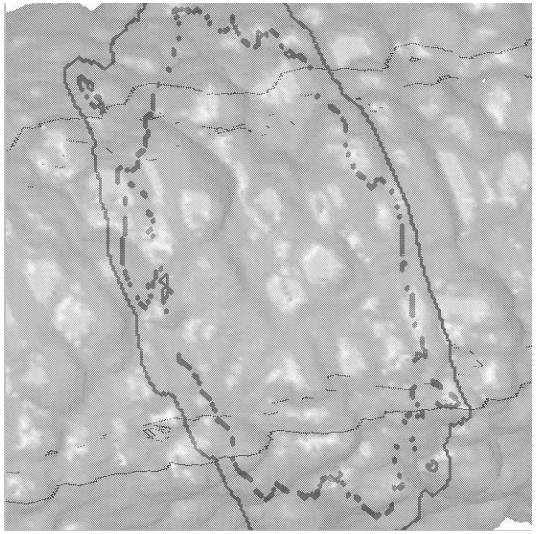

Slow Jet (v=1.0e9 cm/sec)

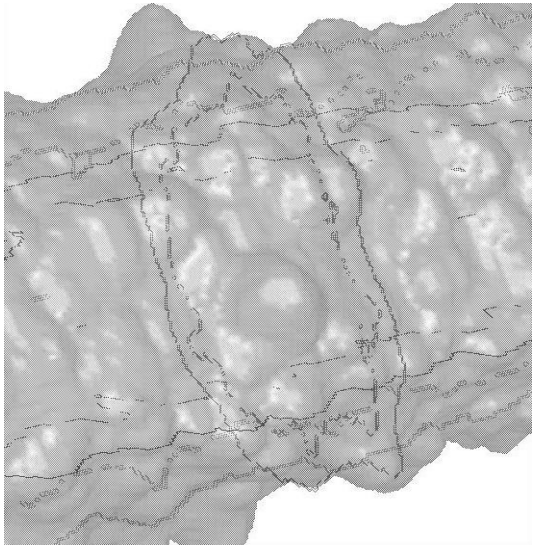

$$\lambda_J \approx \sqrt{\frac{k_B T r^3}{G M \mu}}$$

VH-1 simulations of jet interaction with the ambient medium produces transverse shocks.

Fast Jet (v=1.5e9 cm/s)

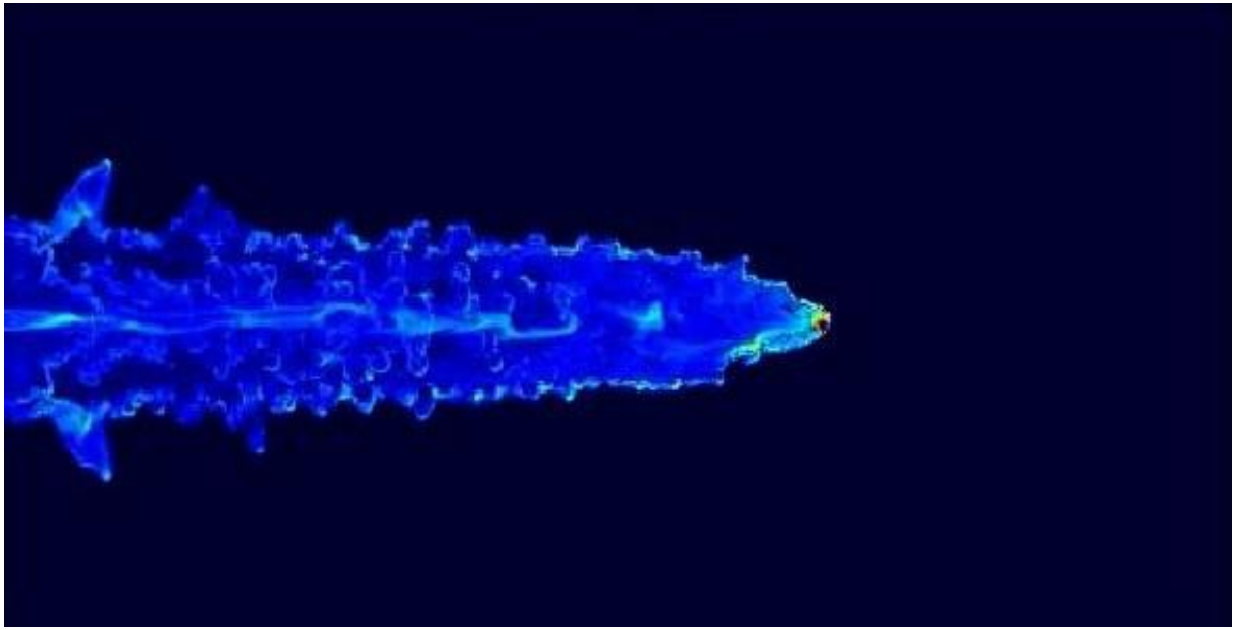

$$\lambda_J \approx \sqrt{\frac{k_B T r^3}{GM\mu}}$$

Detail of transverse shocks generated by jet interaction with the ambient medium.

Fast Jet (v=1.5e9 cm/s)

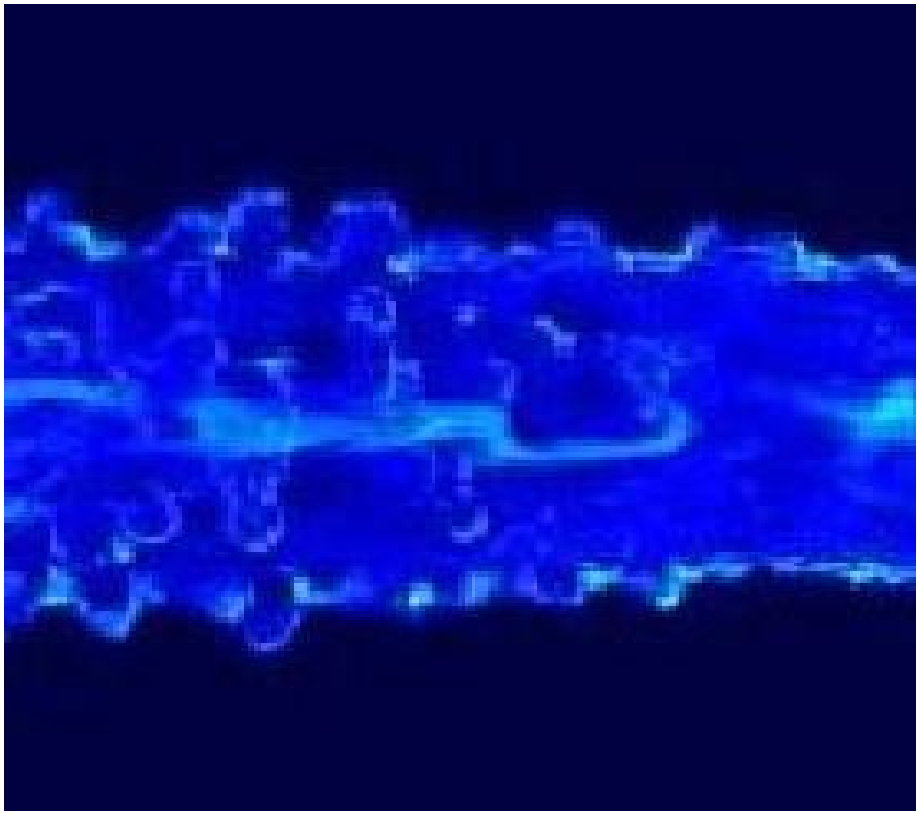

$$\lambda_J \approx \sqrt{\frac{k_B T r^3}{GM\mu}}$$

Pressure equilibrium of B-field with ram pressure from jet taken from hydrodynamics simulations allows for an estimation of magnetic field

$$B^2/8\pi = 1/2\ \rho v^2$$

Ram pressure can also be compared with PIC code estimation of momentum transfer via plasma processes once we obtain estimates for momentum transfer.

Jet-Induced Synchrotron Emission

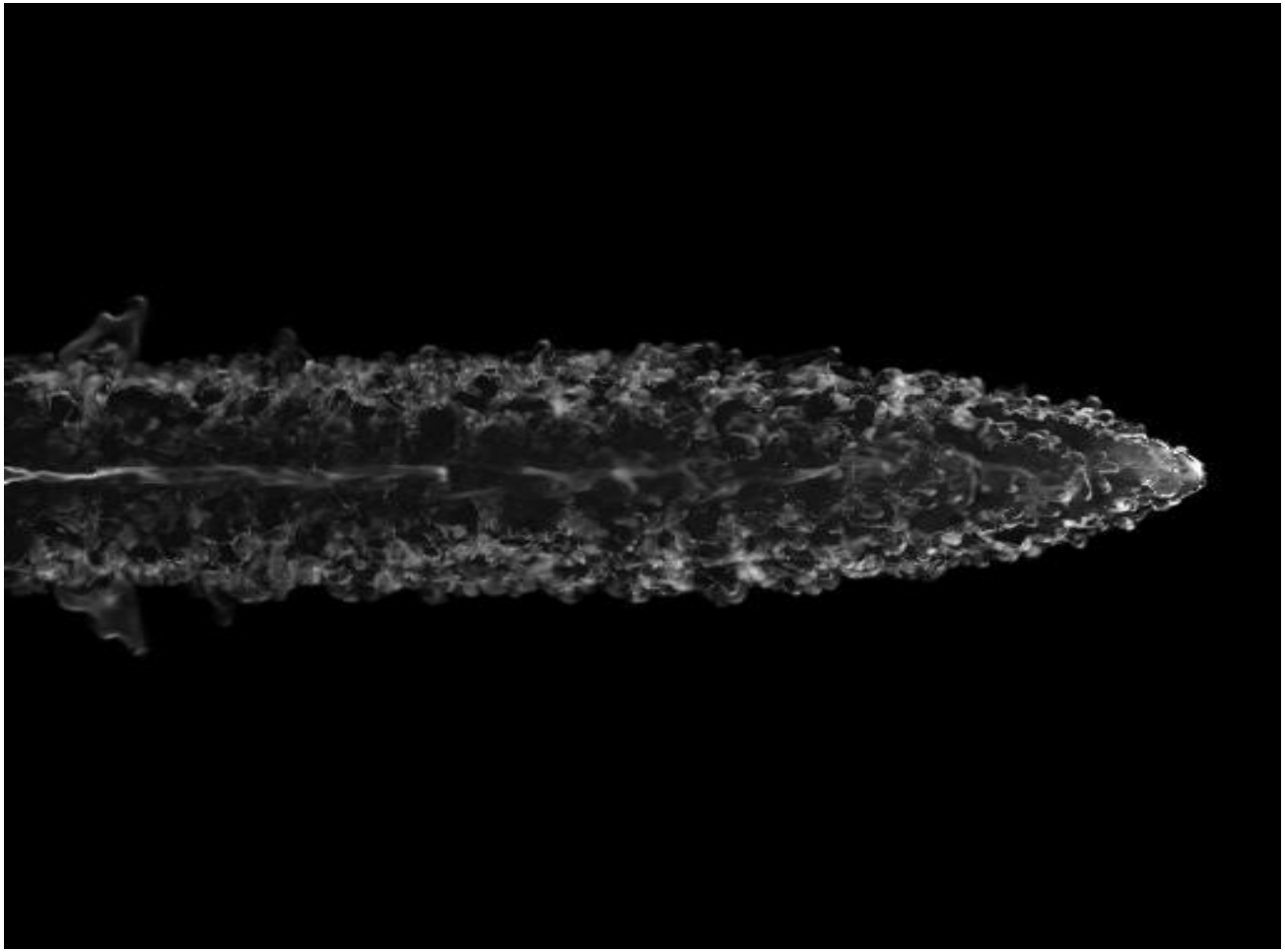

Jet-Induced Synchrotron Emission

Note on modeling:

It is possible to estimate the effects of a magnetic field in the production of synchrotron radiation in this way.

However, a simulation which generates the magnetic fields self-consistently, and one which can fully account for relativistic effects seems like a more reasonable approach.

For this reason, we are moving toward large-scale simulations using a fully relativistic, magneto-hydrodynamic code, and have chosen the PLUTO code (Mignone et al.) for this effort. The code is highly modularized. After we benchmark PLUTO with the VH-1 results, we will move to incorporate plasma processes in the PLUTO code.

Relativistic Magnetohydrodynamics (RMHD) Module

$$
\begin{aligned}
\frac{\partial D}{\partial t} + \nabla \cdot (D\mathbf{v}) &= 0 \\
\frac{\partial \mathbf{m}}{\partial t} + \nabla \cdot \left(w_{tot}\gamma^2 \mathbf{v}\mathbf{v} - \mathbf{b}\mathbf{b} + p_{tot}\mathbf{I} \right) &= 0 \\
\frac{\partial E}{\partial t} + \nabla \cdot \mathbf{m} &= \Lambda \\
\frac{\partial \mathbf{B}}{\partial t} + \nabla \times (\mathbf{v} \times \mathbf{B}) &= 0 \\
\frac{\partial \rho X_k}{\partial t} + \nabla \cdot (\rho X_k \mathbf{v}) &= S_k
\end{aligned}
$$

$$
\mathbf{m} = w_{tot}\gamma^2 \mathbf{v} - \gamma(\mathbf{v}\cdot\mathbf{B})\mathbf{b}\,, \quad w_{tot} = w + |b|^2
$$

$$
\mathbf{b} = \mathbf{B}/\gamma + \gamma(\mathbf{v}\cdot\mathbf{B})\mathbf{v}\,, \quad |b|^2 = \mathbf{B}^2/\gamma^2 + (\mathbf{v}\cdot\mathbf{B})^2
$$

Code is modularized: HD, RHD, RMHD share features (Mignone et al.)

Initial Run of Relativistic MHD Code PLUTO on NRL SGI Altix Machines.

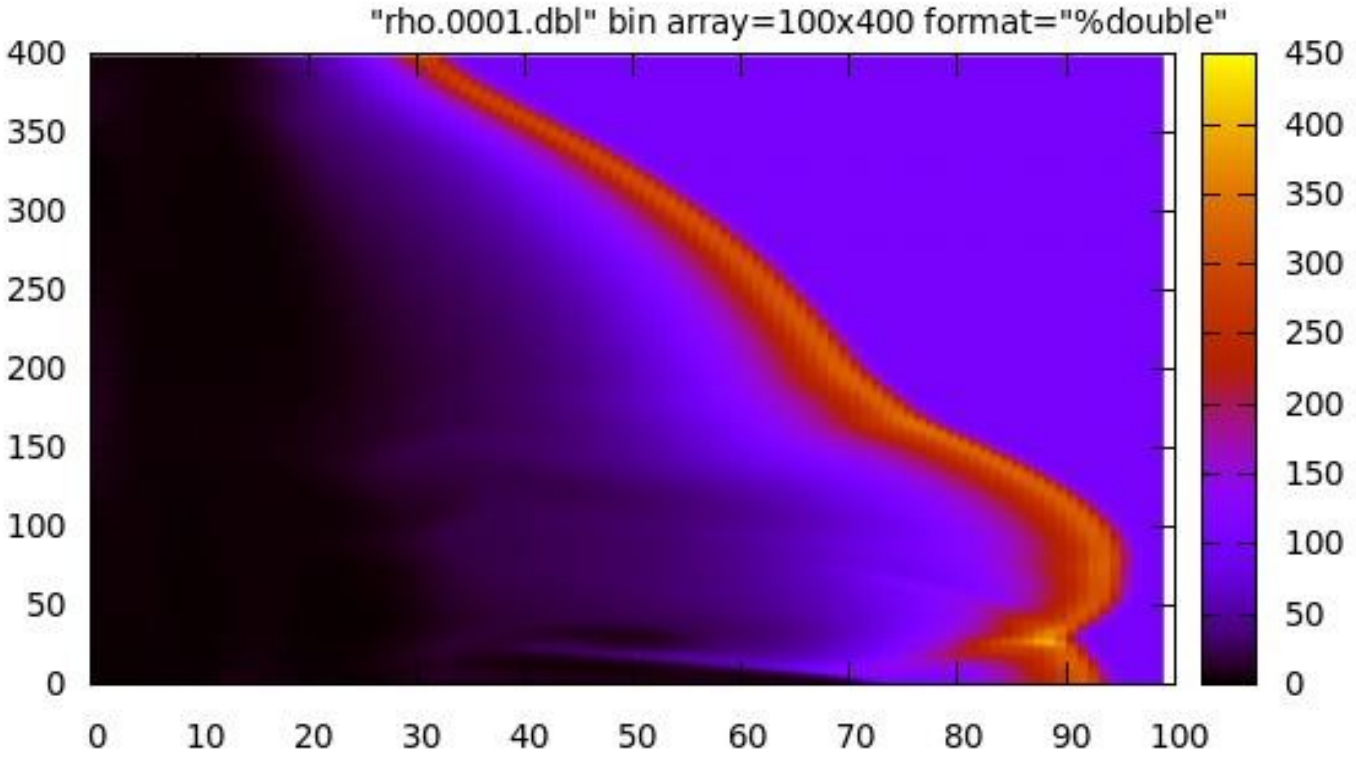

PLUTO Relativistic Magneto-Hytrodynamic Code Initial Results

axial symmetry, jet v/c=.995, jet density

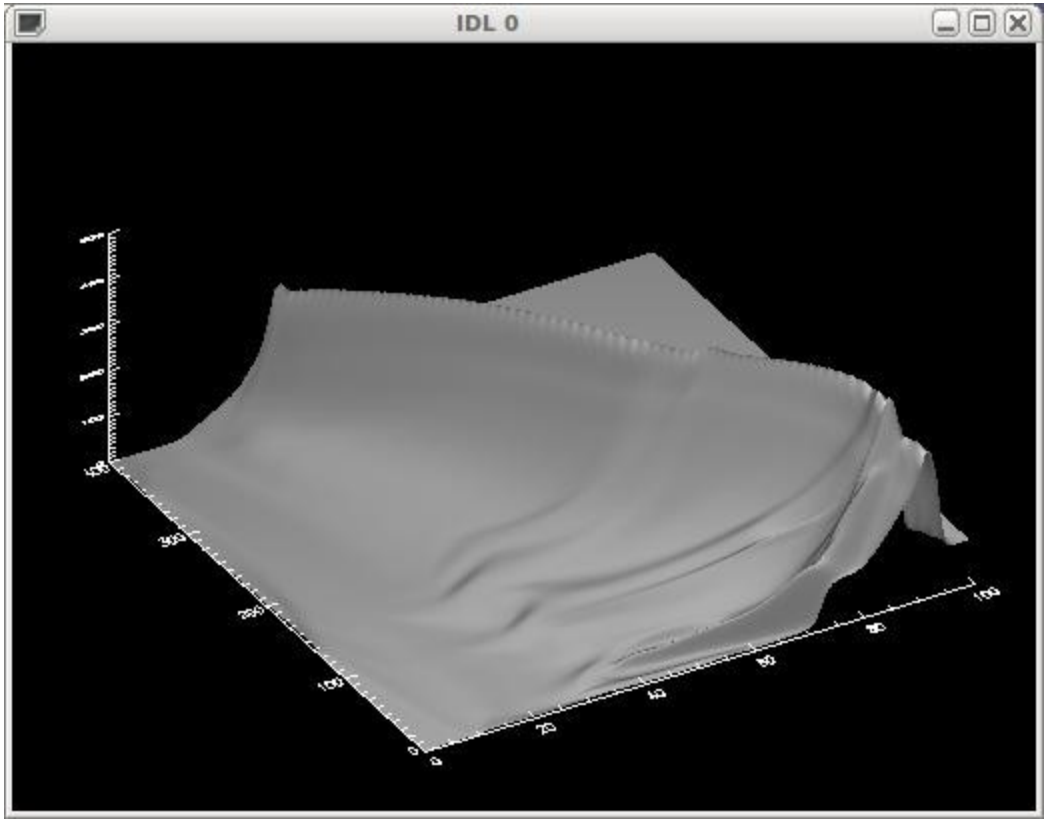

PLUTO Relativistic Magneto-hytrodynamic Code Initial Results

axial symmetry, jet v/c=.995, pressure

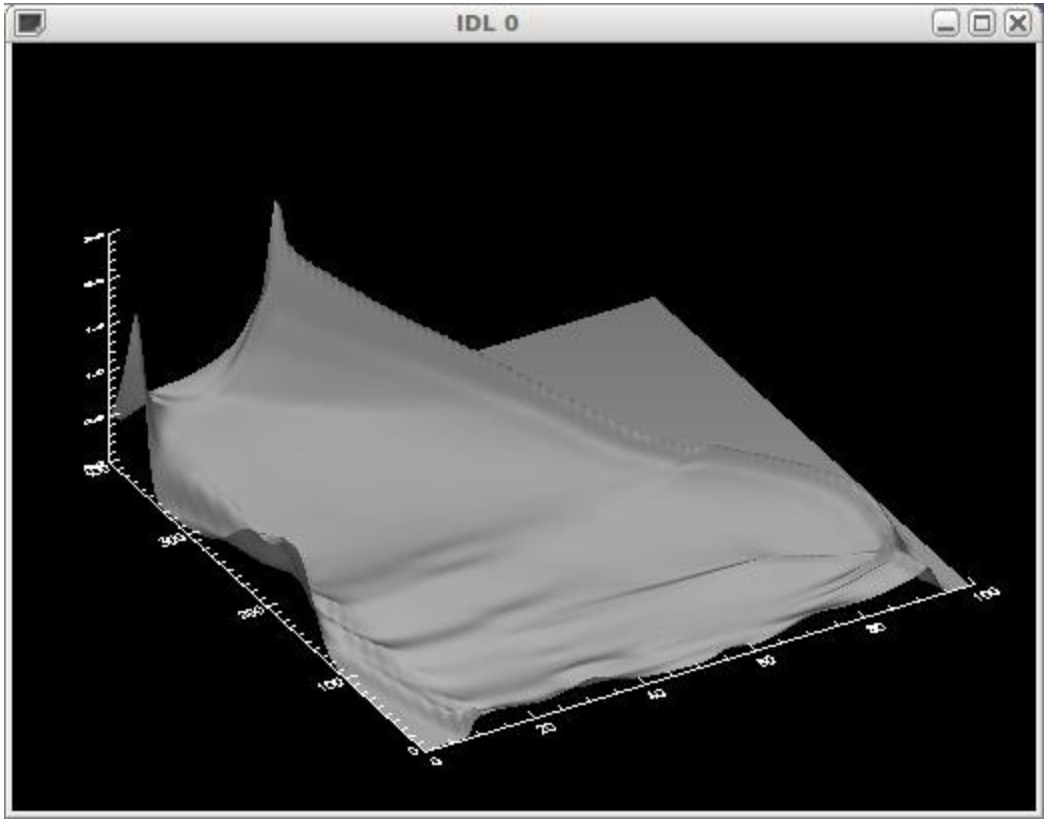

PLUTO Relativistic Magneto-Hydrodynamic Code Initial Results:

axial symmetry, jet v/c=.995, axial velocity

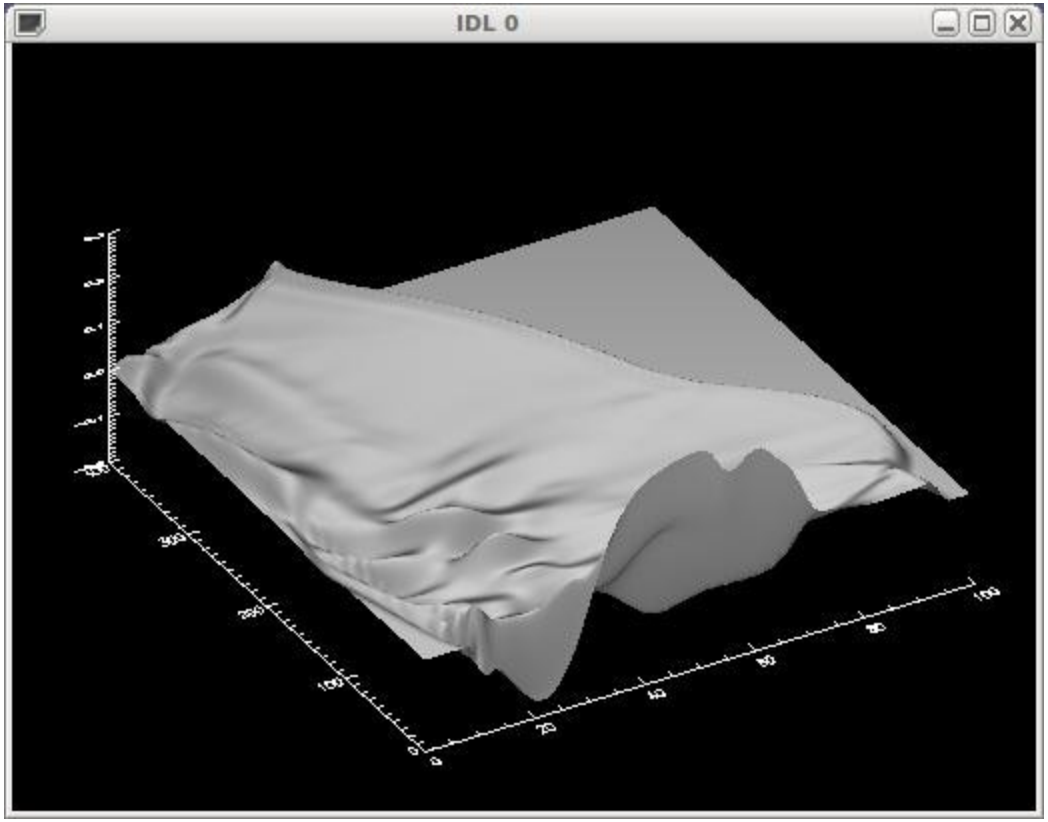

PLUTO Relativistic Magneto-Hydrodynamic Code Initial Results: axial symmetry, v/c-.995, radial velocity

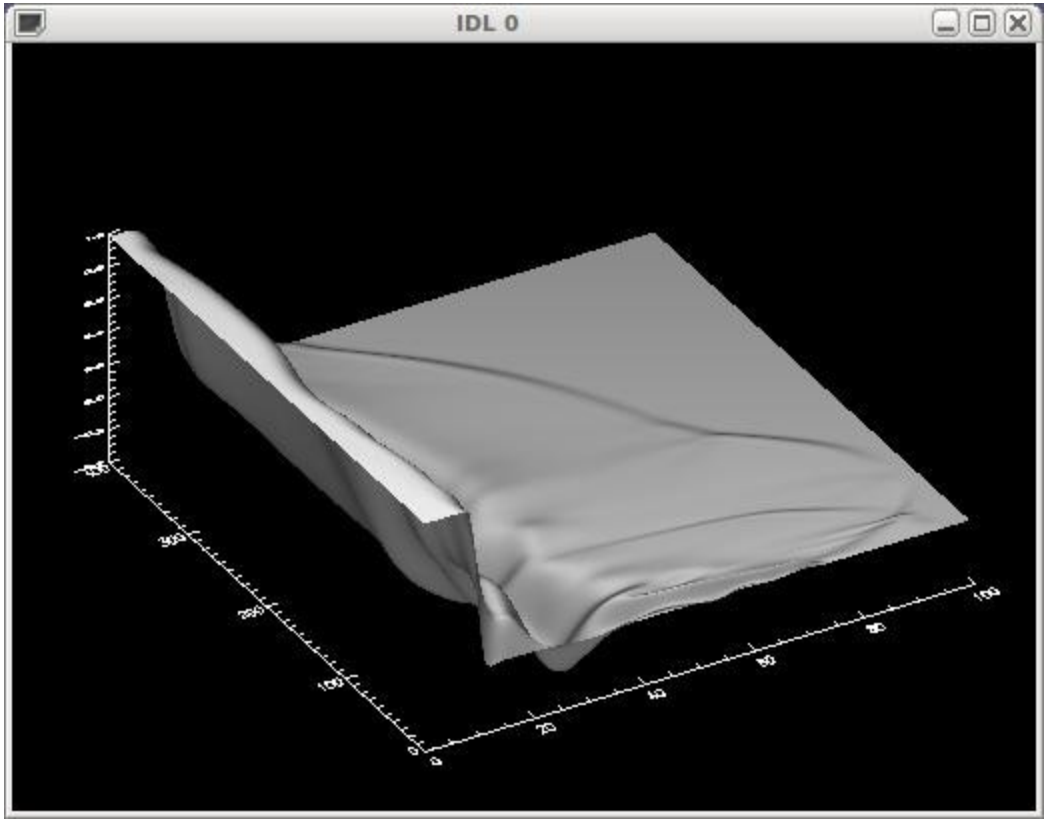

Concluding Remarks:

Particle-in-cell simulations of electron-proton jet interacting with an ambient medium yield:
- energy deposition rate
- momentum transfer rate

consistent with wave-population code model.

Plasma processes are the dominant energy loss mechanism for most astrophysical scenarios.

We need to determine whether or not plasma processes are the dominant momentum transfer mechanism. This seems likely, and we are proceeding on this project.

We have underway a multi-scale code effort to incorporate plasma processes as energy and momentum drivers for the evolution of astrophysical jets modeled by a parallelized VH-1 hydrodynamics code and the PLUTO relativistic magneto-hydrodynamics code.

Thanks for your attention!

PIC Code Simulations to confirm Robinson and Newman (1990)

LSP PIC Code 2D Simulation Model:

- 2D (x,y) Cartesian simulation box with periodic boundary conditions on all 4 sides.
- The box is $128\lambda_{De}$ x 128 λ_{De}, with $\Delta x=\Delta y=\lambda_{De}$.
- LSP is initialized with "real" quantities, so I select $n_e=1$ cm^{-3}, $T_e=861$ eV, and $\Delta x=2180$ cm (satisfying the grid heating constraint $\Delta x<\pi\lambda_{De}$)
- Following [Newman:1990], $T_i=0.01T_e$, and we use 9 macro-particles per species, per simulation cell (Newman *et al*. use 8).
- The ion density depression is initialized according to Eq. (4) of [Newman:1990]: $$n_i = n_e - a_0 \frac{rw^3}{\left(w^2+r^2\right)}\cos\theta$$ where $w=28\lambda_{De}$ is the characteristic width of the induced wave packet, and θ is the angle relative to the x axis [$r=(x^2+y^2)^{1/2}$].
- The LSP simulation is initialized with n_e uniform in all space, and we carry out a Poisson solution for the E-fields at t=0 before switching to an explicit EM field solution at all later times.
  - Newman et al. are using an electrostatic solver (although they don't state a specific method of solution) with an extended particle model that is probably like the Birdsall cloud-in-cell model (Birdsall:1991) .

Test Case: no density depression

- Newman et al. quote a fluctuation level for electrostatic waves in their PIC simulation of <W>~0.002. Our simulation without an initial density depression gives <W>~0.00024 (about a factor of 8 smaller). I attribute this mainly to our extended (or cloud-in-cell) model which has been fine-tuned over the years by R. E. Clark and D. R. Welch beyond the original Birdsall description. We are also using the Godfrey and Goplen time-bias algorithm [Godfrey:1980] during the EM field solve at a small level to main very good energy conservation (<1%).

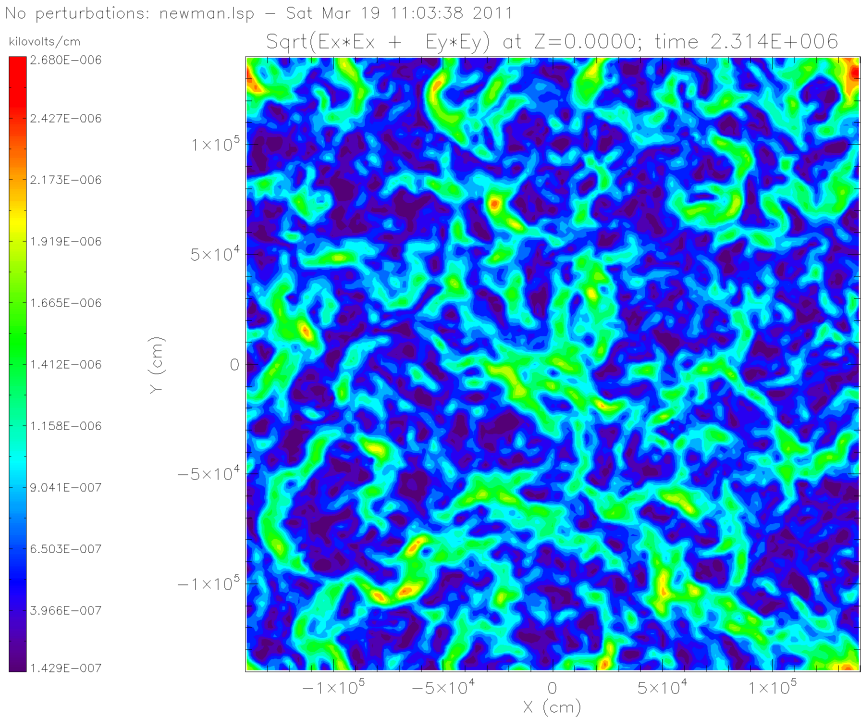

Electrostatic field magnitude after 130 $\omega_p t$ for the case without an initial density depression (newman01).

Case with a 5.5% density depression:

- Following [Newman:1990] again, we have run a case with m_i/m_e=100 and a peak initial density depression of ~5.5% (Newman et al. used something closer to 6%).

Initial ion density contours:

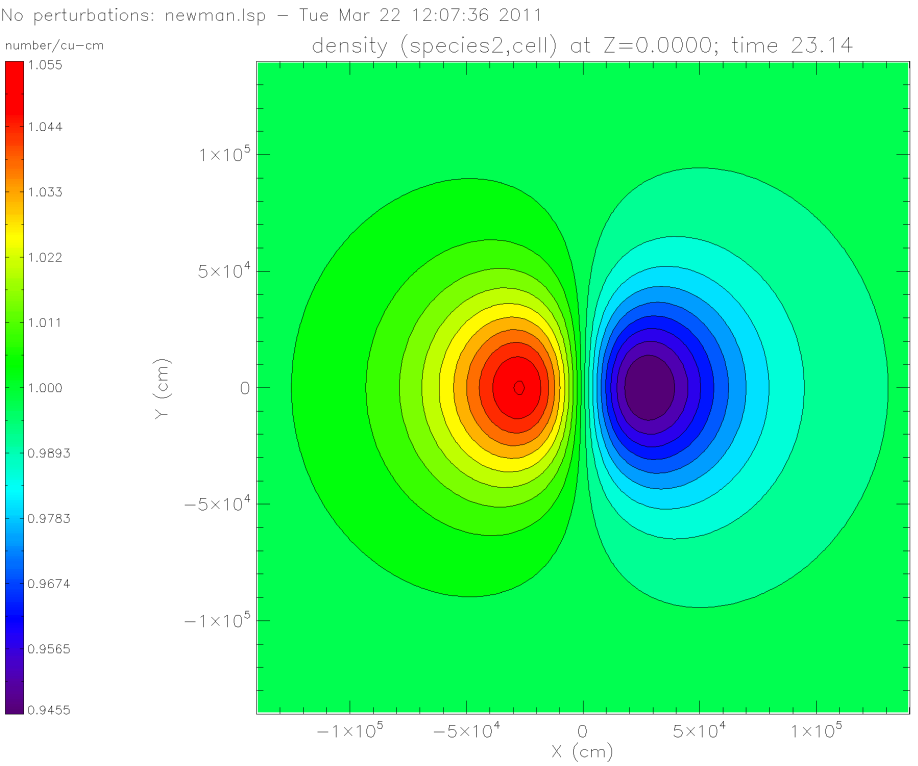

Initial net charge density contours:

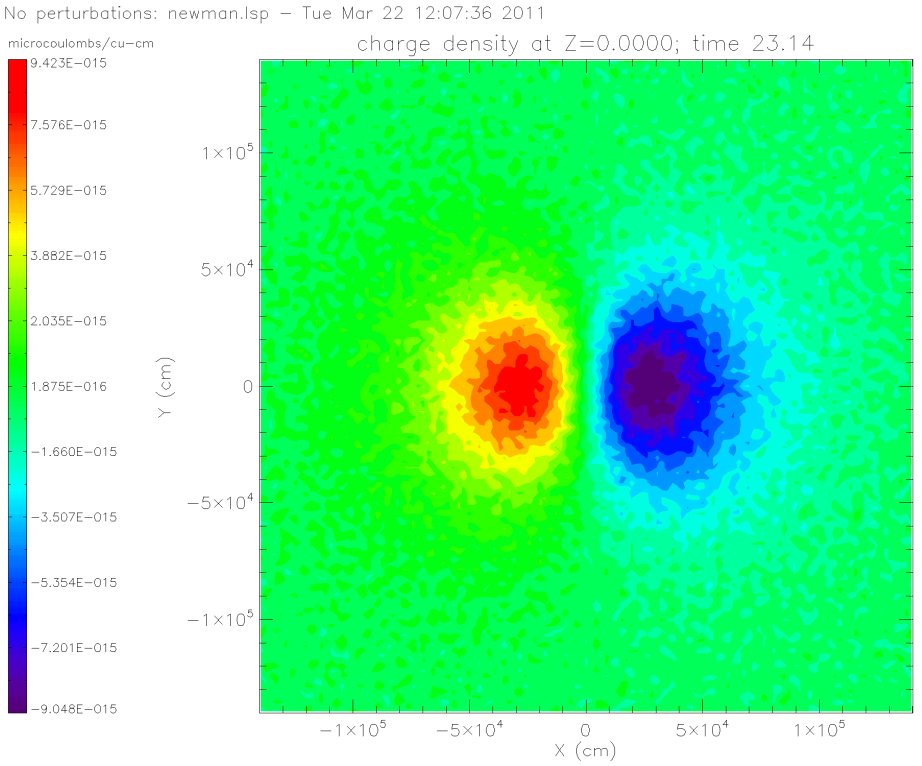

Using LSP PIC code, we confirm the Robinson and Neuman simulations, but with modern PIC methods and a much larger number of particles.

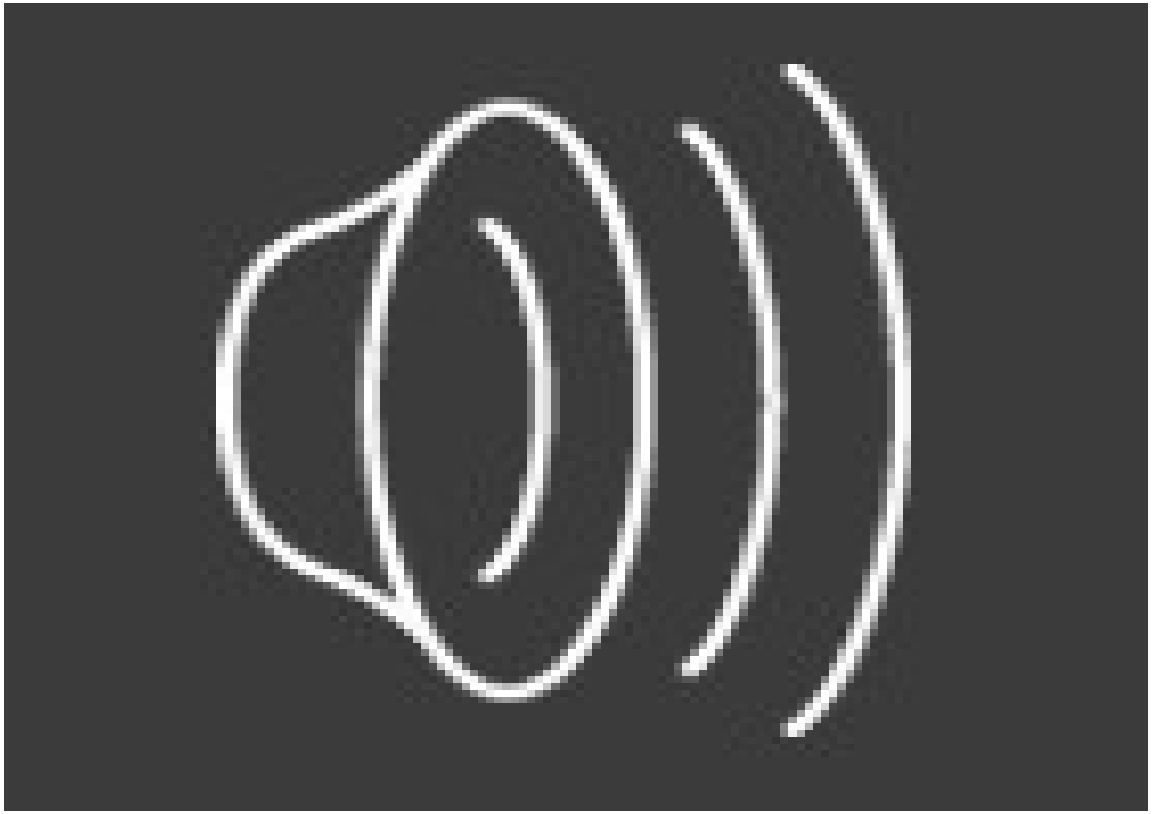

Hadronic-Jet-Ambient-Medium γ–ray Spectrum: fully anisotropic calculation

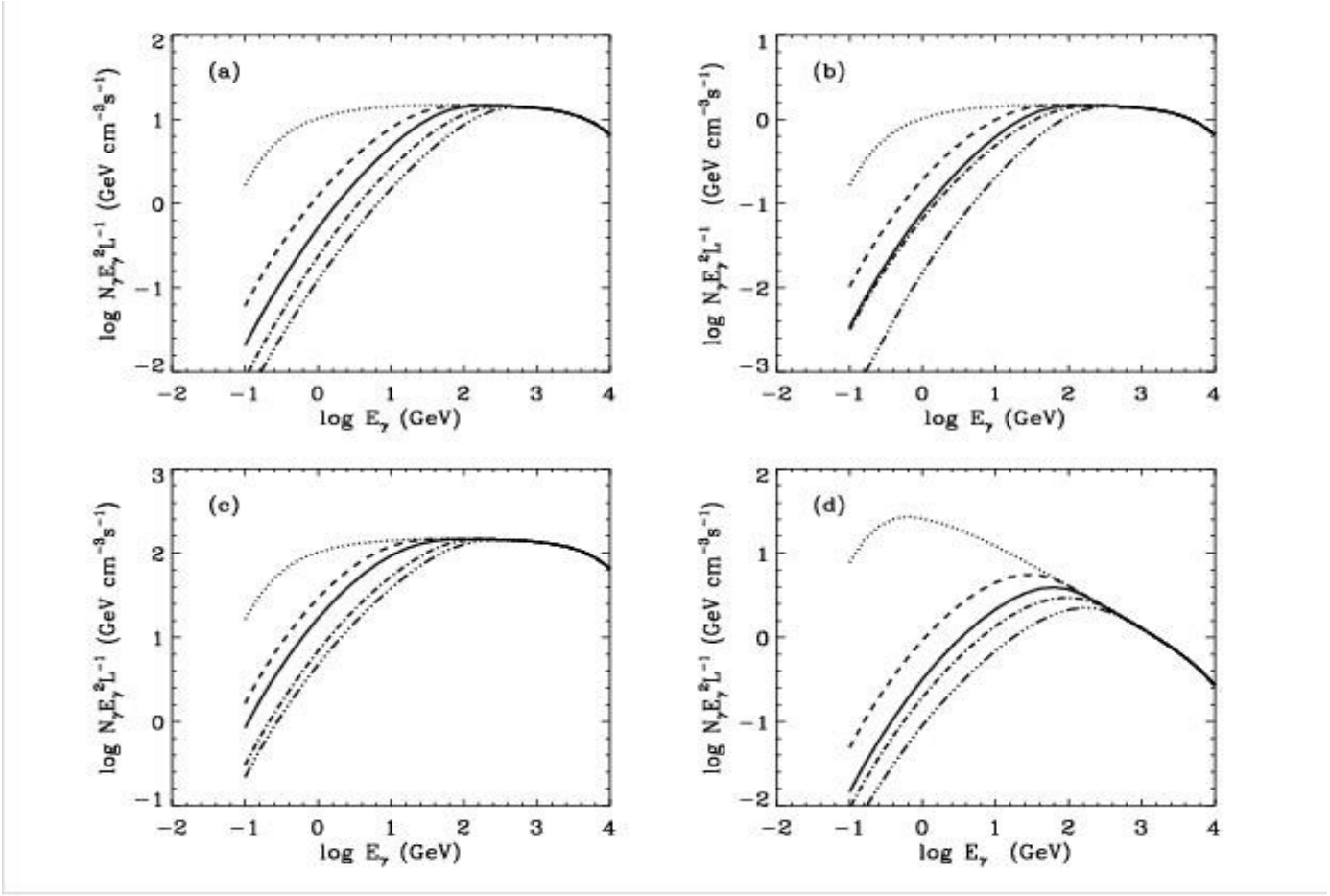

Beall and Bednarek, Ap.J.1999, 510, 188.

Newman05-ES:

Ion Density at center of box:

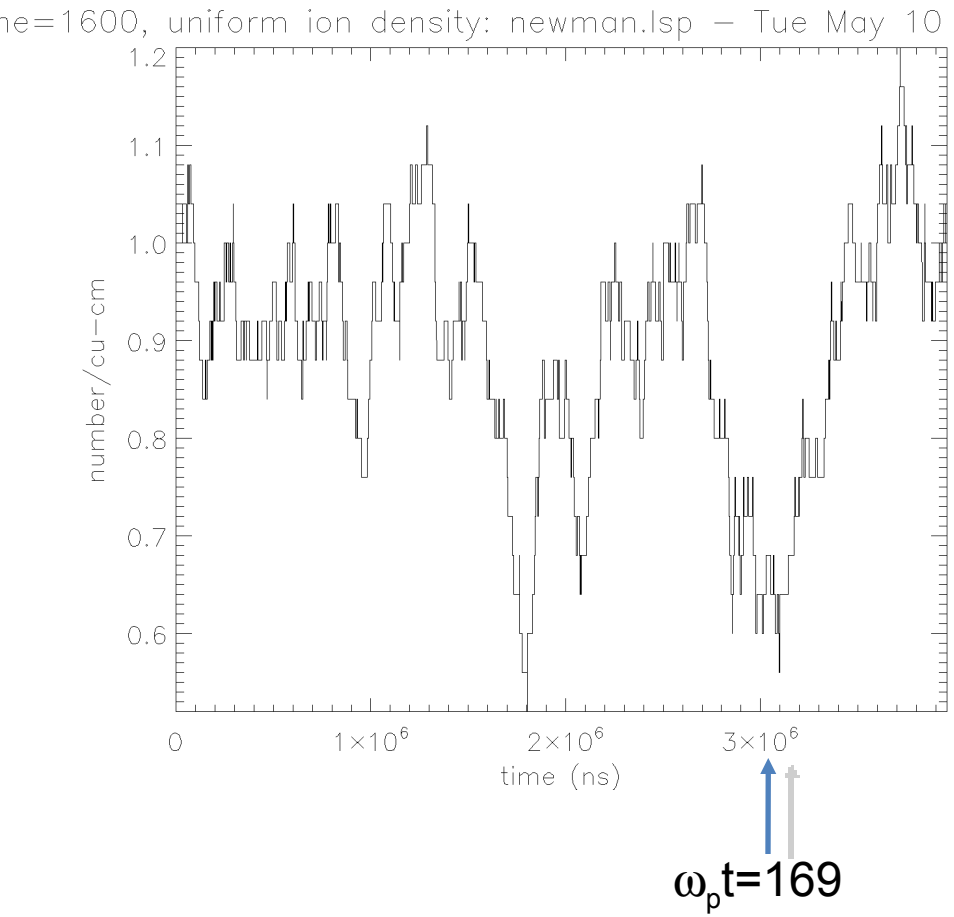

$\omega_p t=169$

Electron Density at center of box:

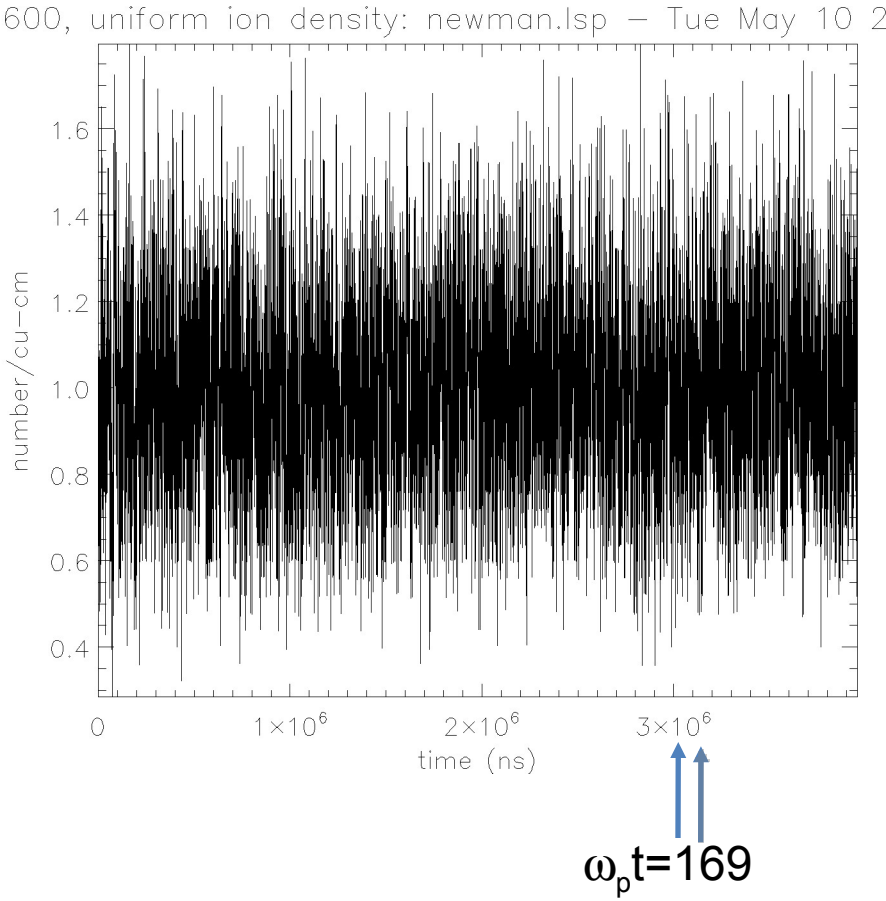

$\omega_p t=169$

Ex field component at center of box:

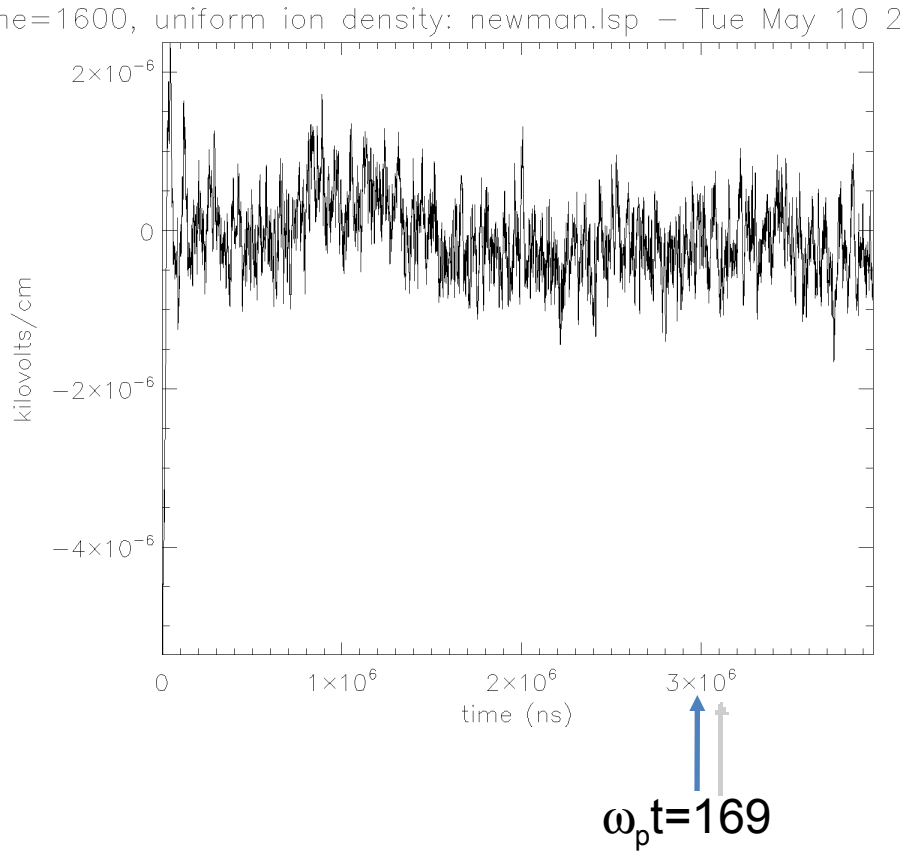

$\omega_p t=169$

Charge density at center of box:

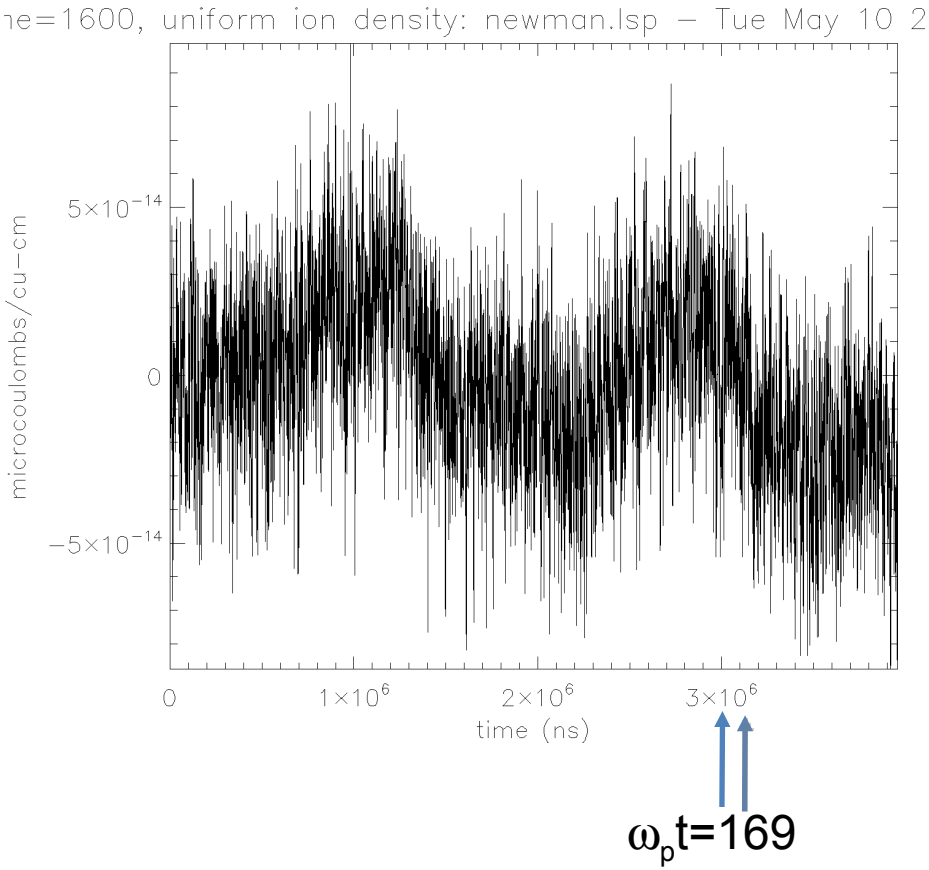

$\omega_p t=169$

References:

[Birdsall:1991] C. K. Birdsall and A. B. Langdon, Plasma Physics Via Computer Simulation (Adam Hilger, Bristol, 1991), p. 20.

[Godfrey:1980] B. B. Godfrey and B. C. Goplen, Bull. Am. Phys. Soc., "Practical evaluation of time-biased electromagnetic field algorithm for plasma simulations," **25**(8),854 (1980).

[Newman:1990] D. L. Newman, R. M. Winglee, P. A. Robinson, J. Glanz and M. V. Goldman, "Simulation of the collapse and dissipation of Langmuir wave packets," Phys. Fluids B **2**, 2600 (1990).

We are exploring caviton formation and dynamics with fully kinetic particle-in-cell (PIC) simulations:

- The calculations presented here model relativistic electron-positron beam propagation through an electron-proton background plasmas
- The PIC simulations follow the growth and saturation of an initially cold electron-positron beam undergoing unstable two-stream oscillations.
- Coupling to the background plasma electrons and ions through three-wave processes leads to the formation of ion waves and cavitons, beginning at the time of the initial saturation of the two-stream mode, and continuing thereafter.
- We are analyzing these simulations to study several issues related caviton dynamics, including momentum transfer from the cavitons to the background thermal plasma and energetic electron and proton acceleration.

PIC simulation model of jet showing caviton formation and momentum transfer:

- 1D, length L = 6×10^6 cm
- Periodic boundaries.
- L > maximum two-stream unstable wavelength.
- Ratio of plasma to beam densities = $n_{pe}/n_{be} = 20$, $n_p = 1$ cm^{-3}
- Beam velocity, $v_b = 0.866c$
- Grid resolution ~0.2xDebye-length to resolve caviton structures.
- This calculation is computationally intensive.

Beam-plasma interaction converts a cold beam into a thermal e^+-e^- stream interpenetrating the background plasma

Field energy vs. t:

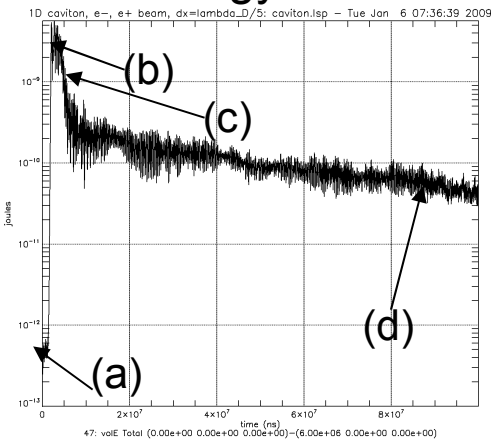

Electron and positron total kinetic energy:

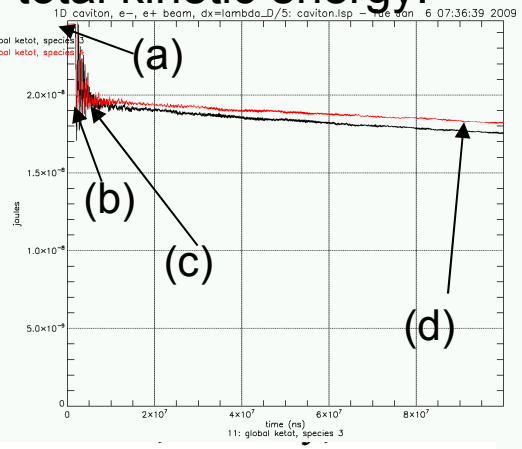

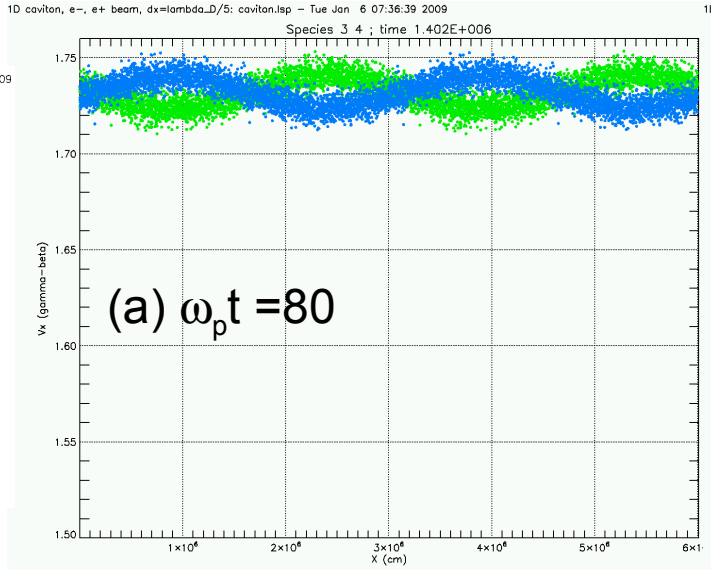

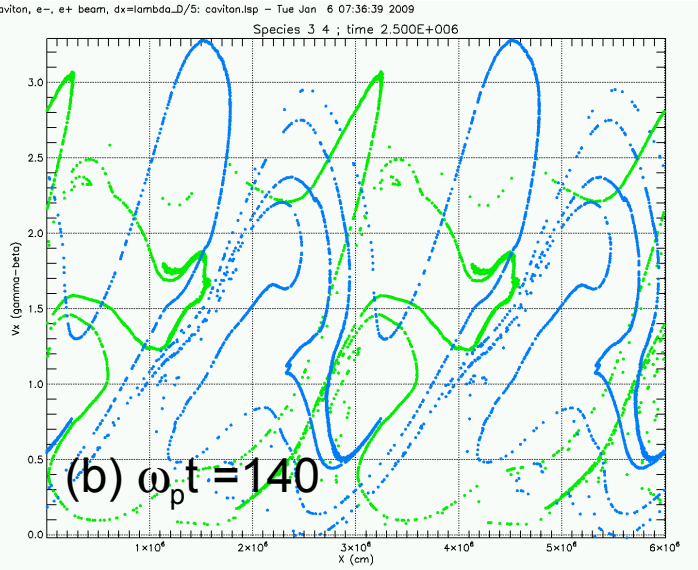

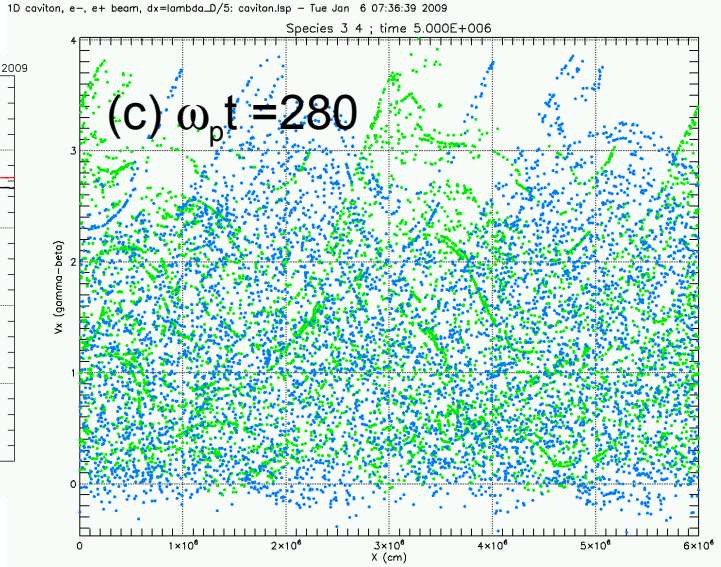

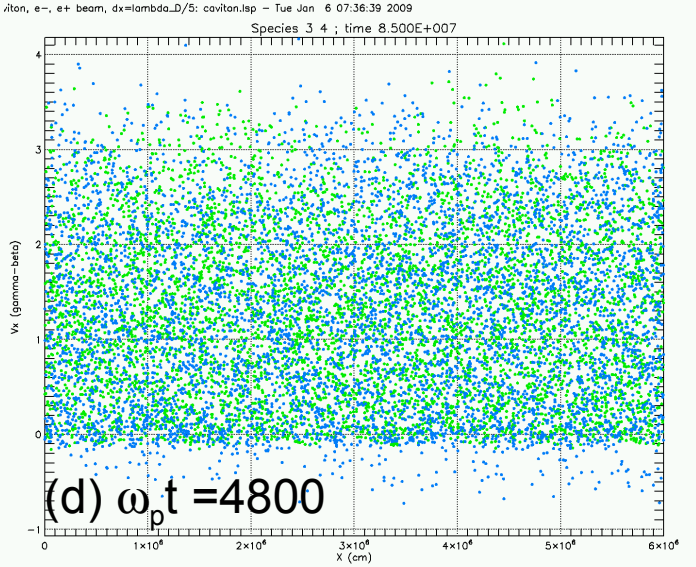

2. Particle-in-cell simulation of electron-proton jet interacting with a fixed magnetic field

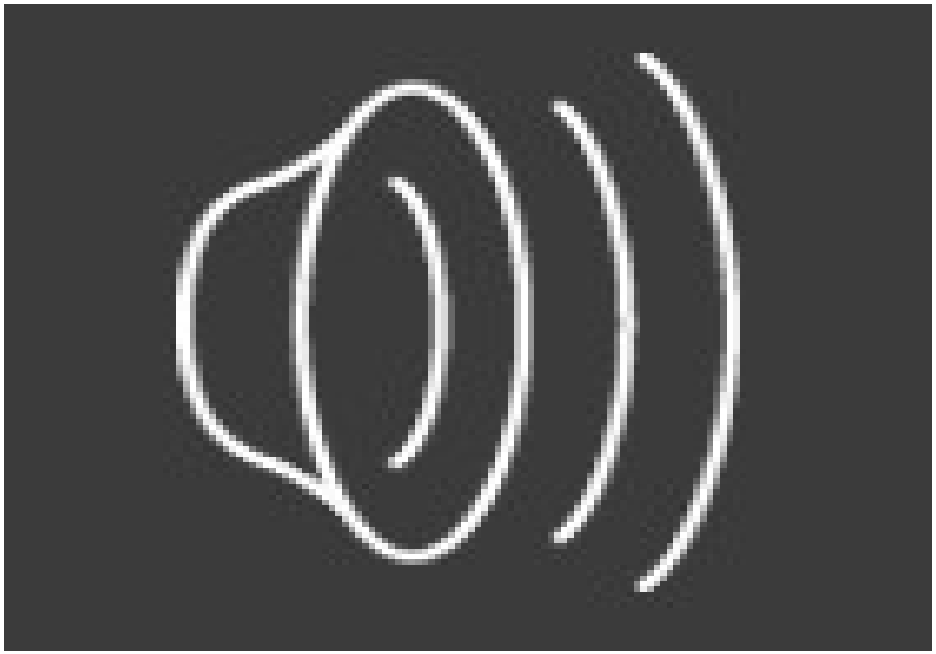

Jet-Ambient Medium Interaction

The primary energy loss mechanism for the electron-positron jet is via plasma processes:

- The two stream instability
- The oscillating two stream instability
- Ion-acoustic waves

These instabilities set up waves in the plasma which produce regions of high electric field strength and relatively low density, called “cavitons” (after “solitons” or solitary waves), which propagate like wave packets in quantum mechanics.

These mix, collapse, and reform, depositing energy into the ambient medium, transferring momentum to it, and entraining (i.e., dragging along and mixing) the ambient medium within the jet.